Received: 19 April 2023 | Revised: 25 September 2023 | Accepted: 9 October 2023

DOI: 10.1002/wnan.1935

ADVANCED REVIEW

WIREs NANOMEDICINE AND NANOBIOTECHNOLOGY WILEY

Receptor for advanced glycation end-products: Biological significance and imaging applications

Iwona T. Dobrucki[1,2,3,4] | **Angelo Miskalis**[1] | **Michael Nelappana**[1,2] | **Catherine Applegate**[2,5] | **Marcin Wozniak**[2,6] | **Andrzej Czerwinski**[2] | **Leszek Kalinowski**[2,6,7] | **Lawrence W. Dobrucki**[1,2,3,5,6]

[1]Department of Bioengineering, University of Illinois at Urbana-Champaign, Urbana, Illinois, USA

[2]Beckman Institute for Advanced Science and Technology, Urbana, Illinois, USA

[3]Department of Biomedical and Translational Sciences, Carle-Illinois College of Medicine, University of Illinois at Urbana-Champaign, Urbana, Illinois, USA

[4]Academy of Medical and Social Applied Sciences, Elblag, Poland

[5]Cancer Center at Illinois, Urbana, Illinois, USA

[6]Division of Medical Laboratory Diagnostics—Fahrenheit Biobank BBMRI.pl, Medical University of Gdansk, Gdansk, Poland

[7]BioTechMed Centre, Department of Mechanics of Materials and Structures, Gdansk University of Technology, Gdansk, Poland

Correspondence
Lawrence W. Dobrucki, Department of Bioengineering, University of Illinois at Urbana-Champaign, 405 N. Mathews Ave, MC-251, Urbana, IL 61801, USA.
Email: dobrucki@illinois.edu

Funding information
Cancer Center at Illinois; Polish Ministry of Education and Science, Grant/Award Numbers: DIR/WK/2017/01, 10/E-389/SPUB/SP/2020

Edited by: Dipanjan Pan, Associate Editor and Gregory Lanza, Editor-in-Chief

Abstract

The receptor for advanced glycation end-products (RAGE or AGER) is a transmembrane, immunoglobulin-like receptor that, due to its multiple isoform structures, binds to a diverse range of endo- and exogenous ligands. RAGE activation caused by the ligand binding initiates a cascade of complex pathways associated with producing free radicals, such as reactive nitric oxide and oxygen species, cell proliferation, and immunoinflammatory processes. The involvement of RAGE in the pathogenesis of disorders such as diabetes, inflammation, tumor progression, and endothelial dysfunction is dictated by the accumulation of advanced glycation end-products (AGEs) at pathologic states leading to sustained RAGE upregulation. The involvement of RAGE and its ligands in numerous pathologies and diseases makes RAGE an interesting target for therapy focused on the modulation of both RAGE expression or activation and the production or exogenous administration of AGEs. Despite the known role that the RAGE/AGE axis plays in multiple disease states, there remains an urgent need to develop noninvasive, molecular imaging approaches that can accurately quantify RAGE levels in vivo that will aid in the validation of RAGE and its ligands as biomarkers and therapeutic targets.

This article is categorized under:

Diagnostic Tools > In Vivo Nanodiagnostics and Imaging

Diagnostic Tools > Biosensing

KEYWORDS

AGE, AGER, fluorescence, molecular imaging, PET, RAGE, SPECT

Iwona T. Dobrucki and Angelo Miskalis contributed equally to this study.

1 | INTRODUCTION

Receptor for advanced glycation end-products (RAGE, AGER) is a 50–55 kDa membrane-bound immunoglobulin surface receptor discovered in 1992 by Schmidt et al. after searching for receptors that mediate interactions between the advanced glycation end-products (AGEs) and endothelium (Neeper et al., 1992; A. M. Schmidt et al., 1992). The protein is expressed by the AGER gene located on chromosome 6 in the major histocompatibility complex three (MHC III) region. RAGE pre-mRNA has 11 exons spaced by 10 introns, which, depending on splicing, can produce different RAGE isoforms (Chuah et al., 2013; Sterenczak et al., 2013; Sugaya et al., 1994). Complete RAGE consists of an extracellular ligand-binding domain, a single-helix transmembrane area, and a cytoplasmic tail as depicted in Figure 1 (Bongarzone et al., 2017; Xie et al., 2008). The extracellular region includes three specific regions: a flexible, positively charged variable (V) domain, a positively charged constant (C1) domain, and a negatively charged C2 domain (Bongarzone et al., 2017; Fritz, 2011; Yatime & Andersen, 2013).

RAGE can oligomerize with its extracellular and transmembrane domains, which is crucial for ligand binding and activating the receptor's signaling pathways (Xue et al., 2011; Yatime & Andersen, 2013). Within its cytoplasmic domain, ligand-stimulated RAGE can interact with intracellular effectors such as the formin diaphanous 1 (DIAPH1), mitogen-activated protein kinases (MAPK) such as extracellular signal-regulated kinase 1/2 (ERK-1/2), and dedicator of cytokinesis protein 7 (DOCK7) (Bongarzone et al., 2017; Sakaguchi et al., 2011; Shekhtman et al., 2017; Zhu & Smith, 2019). These interactions can lead to the upregulation of several factors, including nuclear factor κ-light-chain enhancer of activated B cells (NF-κB) and cAMP response element-binding (CREB) protein, resulting in increased RAGE expression, which is associated with a myriad of biological effects (Bongarzone et al., 2017; Ann Marie Schmidt et al., 2000; Sousa et al., 2000).

Due to alternative splicing, RAGE exists in multiple isoforms as depicted in Figure 1 (Ann Marie Schmidt et al., 2000). For example, N-truncated RAGE (N-RAGE) does not possess the V-domain, inhibiting any ligand activity within this domain (Koyama et al., 2007; Sugaya et al., 1994). In contrast, a dominant-negative RAGE (DN-RAGE) consists of the receptor without the cytoplasmic region, preventing downstream signaling activity (Fritz, 2011; Ann Marie Schmidt et al., 2000; Takeuchi et al., 2013). A soluble RAGE (sRAGE), which only includes the extracellular region, can be formed through alternative splicing cleavage of full RAGE by matrix metalloproteinases (MMPs) or G protein-coupled receptors (GPCRs) (Metz et al., 2012; Ling Zhang et al., 2008). Similar to DN-RAGE, the lack of cytoplasmic activity of sRAGE prevents the biological activity from interacting with RAGE ligands. Instead, sRAGE can scavenge RAGE ligands in the extracellular matrix (ECM) and act as a decoy receptor.

RAGE, through its three domains, binds to a diverse range of ligands, including AGEs. AGEs, including Nϵ-carboxymethyl-lysine (CML), Nϵ- carboxyethyl-lysine (CEL), and methylglyoxal (MG) modified proteins, are formed through the irreversible nonenzymatic Maillard reaction between proteins and carbohydrates (Ott et al., 2014). Both CML and CEL levels are elevated in the Western diet, particularly within processed meats, dairy products, and cereal-derived foods (Delgado-Andrade, 2016). In cooking, techniques like frying and roasting are associated with high AGEs

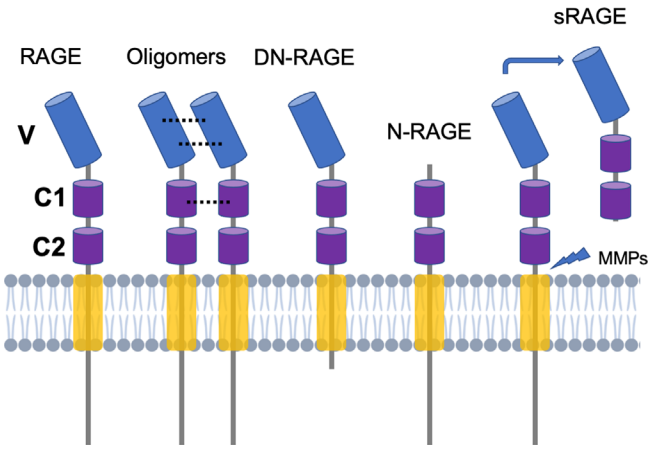

FIGURE 1 Structure of full-length RAGE, including the variable (V) domain, constant (C1 and C2) domains, the transmembrane region, and the cytoplasmic tail. The key RAGE isoforms include (from the left) the full-length RAGE, oligomerized full-length RAGE, dominant negative RAGE (DN-RAGE), N-truncated RAGE (N-RAGE), and soluble (secretory) RAGE (sRAGE).

formation in meats, and fish (Uribarri et al., 2010), which could indicate a causative link between diet and RAGE/AGE axis associated pathologies. Therefore, interactions between RAGE and AGEs are associated with several systemic pathologies including diabetic complications, cancer, and inflammation (Singh et al., 2014; Sparvero et al., 2009). RAGE ligands bind through electrostatic and hydrophobic interactions with the surface of the V-domain, forming V-V homodimers via interlinkage with multiple CML or CEL residues. Fluorescence titration analysis demonstrated that CML and CEL modified small peptides have binding affinities (Kd) of approximately 100 μM to a recombinant RAGE V-domain (Xue et al., 2011). Radiological binding assays showed that CML modified bovine serum albumin (BSA-CML) have a Kd of 10 μM to a monomeric V-domain of RAGE and significantly higher affinity to full-length sRAGE (Kd = 76 nM) (Kislinger et al., 1999; Xie et al., 2008). This is due to the ability of full-length RAGE to oligomerize, bringing multiple V domains together and increasing binding sites. Other RAGE ligands, such as a high mobility group box 1 (HMGB1) and the subtype amphoterin bind to both the C1 and C2 domains with nanomolar affinities (Hori et al., 1995) and are associated with apoptotic and inflammation-related events (Sims et al., 2010; H. Yang et al., 2013). In a number of neurological disorders, it was found that RAGE can also interact with amyloid beta (Aβ) proteins through both the V and C1 domains at nanomolar affinities (Deane et al., 2012; P.-S. Yang et al., 2016). Lastly, RAGE was shown to interact with many of the S100 family of proteins, binding to multiple domains at nano- to micromolar affinities (Bongarzone et al., 2017).

Due to its promiscuous behavior with different ligand types, RAGE overexpression and activity are complexly associated with several pathologies, including cancer, vascular complications, and neurological disorders. Therefore, to better understand the role of RAGE in these pathologies, develop new diagnostic tools and evaluate individualized therapies, there is an immediate need to design clinically translatable, noninvasive imaging approaches targeted at the RAGE/AGE axis that can improve the assessment of receptor activity and validify its biological functions. In the next sections, we will highlight the role of RAGE in physiological disorders, the potential of RAGE/AGE axis-targeted therapeutic interventions and discuss preclinical image-based strategies to assess RAGE quantitatively.

2 | BIOLOGICAL ROLES OF RAGE/AGE AXIS

2.1 | RAGE and cancer

Through interactions with its ligands, RAGE modifies both the tumor and its surrounding microenvironment (TME) in multiple types of cancer, including breast, prostate, glioma, pancreatic, colon cancer, and melanoma (Allmen et al., 2008; Malik et al., 2015; Meghnani et al., 2014; Taguchi et al., 2000). In tumor cells, RAGE activity participates in the progression of these malignancies by enhancing cell proliferation, formation of metastasis, stem-cell-like transitions, survival, and autophagy. Taguchi et al. demonstrated that rat glioma cells cultured in the presence of amphoterin showed increased growth, and removal of RAGE blocked this effect (Taguchi et al., 2000). Immunodeficient mice injected with these activated cells exhibited increased growth, and immunohistochemical analysis showed co-localization with RAGE, amphoterin, and glioma cells, suggesting RAGE-induced tumor growth. In a study by Sharaf et al., the treatment of MDA-MB-231 breast cancer cells with BSA-CML exhibited a significant upregulation in both cell proliferation and invasion through RAGE/AGE mediated signaling (Sharaf et al., 2015). RAGE/AGE activity was associated with increased phosphorylation of ERK-1/2, and p70S6K1 pathways, which has been shown to enhance tumor cell proliferation (Meng et al., 2006; W. Zhang & Liu, 2002). Additionally, it was found that RAGE increased the activity of matrix metalloproteinase-9 (MMP-9), an enzyme strongly linked to promoting tumor aggressiveness by degrading basement-membranes and inducing phenotypes that enhance tumor cell motility (Kessenbrock et al., 2010; Mehner et al., 2014; van't Veer et al., 2002). Moreover, RAGE activity is associated with the induction of the epithelial-to-mesenchymal (EMT) transition, which leads to increased metastasis and tumor inflammation (Brabletz et al., 2018; Kwak et al., 2016). Within the PC-3 prostate cancer cell line, HMGB1/RAGE signaling was shown to increase the EMT markers such as N-cadherin, vimentin, MMP-1, and MMP-10. Also, HMGB1-treated cells demonstrated higher migration rates (J. Zhang et al., 2018). In clinical studies, HMBG1 had higher expression in primary tumor samples for patients with metastatic compared to localized prostate cancer. Yin et al. showed that actions of S100A8/A9 via RAGE caused formation of lung metastasis of MDA-MB-231 cells implanted in an immunocompromised mouse model. In addition, RAGE increased the expression of EMT transcription factors in breast cancer cells ranging from less malignant (MCF-7) to highly metastatic (MDA-MB-231) (Nasser et al., 2015; Yin et al., 2013). Finally, RAGE was also linked

to increased lymph node metastasis within patient tumor samples. All this implicates RAGE as a potential biomarker of poor prognosis and increased tumor aggressiveness.

The expression of RAGE is also correlated with enhanced resistance to antitumor therapies, promoting survival (Huang et al., 2018; Kang et al., 2010; Q.-Y. Zhang et al., 2015). In a study by Kang et al., it was shown that increased RAGE expression in human pancreatic tumor cell lines decreased cell apoptosis when subjected to radiation therapy, chemotherapeutic agents, and hypoxia through autophagy. Importantly, C57BL6 mice inoculated with RAGE knockdown tumor cells showed increased apoptosis and decreased autophagy, indicating its relevance in vivo. These effects were demonstrated in other types of cancer. Recently, Huang et al. demonstrated in vitro and in vivo that RAGE/HMGB1 interactions were responsible for increased autophagy in colorectal cancer through ERK-1/2 phosphorylation of dynamin-related protein 1 (DRP1) (Huang et al., 2018). Interestingly, tissue microarray analysis of patient biopsies showed that a high presence of RAGE G82S polymorphism expression correlated to increased levels of p-DRP1 following chemotherapy treatment. These individuals also had a poorer overall 5-year survival than those without RAGE expression.

These observations affirm the impact of RAGE in promoting therapeutic resistance both in preclinical and clinical studies. In addition to tumor cells, RAGE modulates the TME. One prominent mechanism is the propagation of chronic inflammation, which, in the abundance of innate immune cells like macrophages and neutrophils, can promote tumor growth and survival (de Visseret al., 2006). RAGE interactions with S100 proteins, AGEs, and HMGB1 within both tumor and microenvironmental cells elevate NF-κB activity, increasing the expression of proinflammatory cytokines such as TNF-α, IL-6, and nitric oxide (NO) (Dukic-Stefanovic et al., 2003; Palanissami & Paul, 2018; Sparvero et al., 2009). In a study by Nasser et al., RAGE knockout mice injected with PyMT mouse breast cancer cells showed a decrease in tumor-associated macrophage (TAM) recruitment within biopsied tumors (Nasser et al., 2015). TAMs are a phenotype of macrophages that possess M2 and M1 type characteristics, inducing both pro-inflammatory cytokines and remodeling activation factors like VEGF, IL-10, and TGF-β (J. Kim & Bae, 2016). Also, S100A7/RAGE interactions in an S100A7-DOX-inducible MMTV mouse injected with MVT-1 cells showed increased recruitment of TAMs and blocking of RAGE through sRAGE reduced recruitment and lung metastasis. S100A7 induced mice showed no increase in the recruitment of CD8/CD3/CD4-positive T cells, preventing the inclusion of the active immune system. Along with TAM recruitment, studies suggest that RAGE-induced autophagy increases the formation of neutrophil extracellular traps within the TME, propagating a proinflammatory microenvironment that promotes tumor metastasis through MMP-9 secretion (Boone et al., 2015; Coussens & Werb, 2002; Zha et al., 2020).

Lastly, evidence suggests that RAGE is able to induce angiogenesis within the TME (Ishibashi et al., 2012; Kwak et al., 2016; Lin Zhang et al., 2017). In a study by Chen et al., it was shown that TAMs isolated from RAGE knockout mice implanted with GL261 cells possessed a lower expression of vascular endothelial growth factor-alpha (VEGFα) and MMP-9 (X. Chen et al., 2014). Total tumor VEGFα and microvessel density were significantly lowered in mice with RAGE KO bone marrow donations and reduced to greater extents in RAGE deficient mice. This is likely because of RAGE actions on both the tumor and the surrounding microenvironment. Similar results have also been shown within breast cancer (Kwak et al., 2016). Additionally, it was shown that RAGE silencing within tumor cells reduces VEGFα expression in vitro and in chicken egg embryo implantation studies, suggesting that RAGE modulates angiogenesis through both tumor cells and the TME (Ishibashi et al., 2012; Liang et al., 2011). In summary, RAGE and its ligands play a complex role in modulating the tumor and its microenvironment through driving proliferation, survival, metastasis, inflammation, and angiogenesis.

2.2 | RAGE and neurological disorders

RAGE/AGE axis has been implicated in various neurological disorders through the induction of oxidative stress, apoptosis, and inflammation in both neurons and their surrounding cells (Juranek et al., 2015; J.-J. Lee et al., 2015). One of such neurogenerative disorders, Alzheimer's disease (AD), is associated with the buildup of amyloid plagues consisting of a known RAGE agonist, an Aβ peptide (Paudel et al., 2020). In a study where mice received cerebral injections of Aβ25–35, the treatment with a small molecule RAGE inhibitor, Pinocembrin, reduced Aβ-induced neurotoxicity and attenuated RAGE expression within the cerebral cortex (R. Liu et al., 2012). Through NF-κB activation, RAGE was shown to increase mitochondrial oxidative stress, resulting in neuronal apoptosis. This was also demonstrated in neuroblastoma cells designed to model AD via overexpression of the Swedish mutant form of APP (mAPP) (R. Liu et al., 2012). Blocking RAGE improved cell viability by lowering the expression of oxidative stress markers and

mitochondrial-related apoptosis. In a separate study, the transgenic expression of DN-RAGE within mAPP expressing mice significantly lowered microglial and astrocyte infiltration, which is associated with inflammation (Fang et al., 2010). The increased expression of RAGE on microglial cells led to elevated Aβ peptide formation, inflammatory cytokines, extensive neuronal damage, and impaired memory, demonstrating RAGE's ubiquity. In a recent study, DN-RAGE expression in microglia was found to restore synaptic activity within the entorhinal cortex of mAPP transgenic mice, one of the earliest affected areas of the brain in AD. This indicates the ability of RAGE to affect neuronal synaptic function and its role in early AD (Criscuolo et al., 2017).

Additionally, RAGE is also shown to possess higher expression in brain sections of AD patients, further demonstrating clinical relevance (Lue et al., 2001; Luth, 2004). In amyotrophic lateral sclerosis (ALS) patient samples, the RAGE/AGE axis is shown to elevate microglia/astrocyte activity, releasing pro-inflammatory cytokines and inducing intracellular oxidative stress (Casula et al., 2011; Z. Wang et al., 2002). In addition to RAGE/AGE-associated increase in the expression of proinflammatory cytokines, AGEs are linked to the presence of superoxide dismutase-1 (SOD-1) mutations which render its ROS scavenging ability ineffective, demonstrating the multiple roles RAGE/AGE axis plays in ALS degeneration (Ray et al., 2016; Shibata et al., 2002). RAGE is also implicated in Parkinson's Disease (PD). In mice administered with the PD-inducing neurotoxin 1-methyl-4-phenyl-1,2,3,6-tetrahydropyridine (MPTP), RAGE was associated with increased NF-κB activity and inflammatory cytokines released by nigral dopaminergic neurons. Interestingly, RAGE deficiency was shown to reduce the death of nigral dopaminergic neurons by reducing ROS levels in a manner independent of MPTP metabolism (Teismann et al., 2012). This suggests the role played by RAGE in inducing MPTP neurotoxicity and provides the potential translation of RAGE therapies in PD.

In addition to AD, PD, and ALS disorders, RAGE has been implicated with neuroinflammation, degeneration, and oxidative stress in Crutzfield-Jacobs, Huntington's disease, and diabetic neuropathy (Anzilotti et al., 2012; Bekircan-Kurt et al., 2014; Freixes et al., 2006). Recent evidence complicates RAGE's negative role in neurological pathologies, as it has been demonstrated to promote neurite outgrowth, differentiation, and recovery (Villarreal et al., 2011). In studies by Huttunen et al., N18 mouse neuroblastoma cells treated with nanomolar concentrations of S100B or amphoterin demonstrated an increased neurite outgrowth, cell viability, and expression of neuronal markers through RAGE dependent activity (Huttunen et al., 2000; Huttunen et al., 2002). Interestingly, treatments in the micromolar range increased levels of oxidative stress markers compared to DN-RAGE control. A study by Businaro et al. showed similar effects with S100B in Aβ peptide-induced neurotoxicity where knocking out RAGE mitigated pro-survival effects (Businaro et al., 2006). Within mature granular neuron cultures, knocking out RAGE decreased neurite outgrowth (L. Wang et al., 2008). Lastly, the differentiative and regenerative abilities of RAGE blocking were demonstrated using in vivo models of intracerebral hemorrhage (ICH) and spinal cord injury (Lei et al., 2015; H. Wang et al., 2017). In the former study, RAGE blockage decreased both the presence of pro-inflammatory cytokines and neuronal stem cell proliferation and differentiation during the later stages of ICH. In a later study conducted by this group, RAGE-HMGB1 inhibition shortly after ICH showed beneficial effects, highlighting the complexity of the RAGE-ligand axis (Lei et al., 2015).

In conclusion, RAGE plays a complex and multifaceted role in neurological disorders, including neuroinflammation, oxidative stress, and cellular signaling. While RAGE activation has been linked to several chronic diseases such as AD, PD, and ALS, its precise role in these conditions remains an area of ongoing research. Further studies are needed to fully understand the mechanisms underlying RAGE-mediated effects and to develop RAGE-targeted therapies.

2.3 | RAGE and diabetes-related cardiovascular complications

RAGE is implicated in multiple cardiovascular diseases (CVDs), including atherosclerosis, thrombosis, myocardial infarctions, and vessel calcification (Egaña-Gorroño et al., 2020; Fukami et al., 2014). Type-1 (D1M) and type-2 (D2M) diabetes are linked closely to cardiovascular mortality. Elevated glucose blood levels additionally increase AGE serum concentrations. Through oxidative stress and pro-inflammatory events, RAGE complicates both diabetic and nondiabetic CVDs (Egaña-Gorroño et al., 2020). Postmortem studies show an increase of RAGE and inflammation activity and reduction of sRAGE expression in diabetic/prediabetic patients (Burke et al., 2004; Cipollone et al., 2003; Di Pino et al., 2016). In a study by Koulis et al., diabetic, RAGE expressing mice demonstrated higher plaque area in aortas than RAGE expressing nondiabetic mice and RAGE deficient diabetic/nondiabetic mice (Koulis et al., 2014). Further examination of RAGE expression in bone marrow-derived cells showed that knocking out the RAGE within donor marrow also reduced RAGE expression on aortic smooth muscle

cells (SMCs) and lowered inflammatory cytokines compared to RAGE expression in diabetic mice. Studies by Schmidt et al. show that blockage of RAGE expression by sRAGE decreased atherosclerosis, inflammation, and SMC activation (Bu et al., 2010; Bucciarelli et al., 2002). Within nondiabetic, ApoE null mice, RAGE depletion reduced atherosclerotic events, lowered inflammatory cytokine and VCAM-1 expression, and reduced the expression of S100B in culture (Harja et al., 2008). In addition, sRAGE was demonstrated to be inversely correlated to vascular calcification events in diabetic patients (H. S. Kim et al., 2013). In preclinical in vivo studies on diabetic rats and mice subjected to surgical myocardial infarcts, groups expressing cytoplasmic domain-deleted RAGE showed improved cardiac function, reduced oxidative stress, and necrotic markers following ischemia/reperfusion injury (Bucciarelli et al., 2008). A similar study reported these effects within nondiabetic mice. Our work demonstrated that RAGE expression is elevated within hindlimb ischemia (Konopka et al., 2018). Lastly, it appears hypoxic conditions affect RAGE activity (Shang et al., 2010; Tsoporis et al., 2010). In a study of coronary artery ligation in Sprague–Dawley rats, vascular ligation upregulated RAGE/S100B colocalization and decreased expression of S100A1 (Tsoporis et al., 2010). Interestingly, cardiomyocytes that were cultured in hypoxic conditions showed an increase in S100B/RAGE expression as well as elevated apoptosis, which was mitigated by RAGE deletion. This observation implicates RAGE's role in hypoxia-induced myocyte apoptosis.

3 | RAGE/AGE AXIS-BASED THERAPEUTIC STRATEGIES

Studies presented in the previous section illustrated the multisystem complexity of the RAGE/AGE axis in oncology, neurology, and cardiology, which makes RAGE an exciting target for therapeutic interventions. Because RAGE overexpression is generally associated with adverse effects, most targeted therapies focus on inhibiting RAGE signaling and reducing AGE levels.

3.1 | Small molecule inhibitors

An example of a small molecule inhibitor binding the extracellular domain of RAGE is [3-(4-2-butyl-1-[4-(4-chlorophenoxy)-phenyl]-1H-inidaxole-4-yl-phenoxy)-propyl]-diethylamine (Azeliragon) which was initially developed by TransTech Pharma (Bongarzone et al., 2017). It has a half-life of 9–14 days in young patients and 1–18 days in the elderly. After in vivo administration, it forms three metabolites, one of which is another RAGE inhibitor (Burstein et al., 2019). Azeliragon inhibits binding interactions between RAGE and CML, S100B, and HMGB1 through interacting with the RAGE's V domain. The drug is able to cross the blood–brain barrier (BBB), making it a potential therapeutic target for RAGE-based neurological disorders (Galasko et al., 2014). In a transgenic AD mouse model, oral dosing of the drug caused a reduction of amyloids in the brain and improved cognitive memory function. A Phase I trial of Azeliragon demonstrated no safety concerns for AD patients (Galasko et al., 2014). Double-blinded, placebo-controlled Phase II trial in 399 patients with mild AD treated with 5 mg/day of Azeliragon over an 18-month period demonstrated improvements in cognitive function but no changes in AD biomarker levels (Burstein et al., 2014; Galasko et al., 2014). It was shown that the drug had no significant effect on cardiac function. A Phase III trial of 5 mg/day was conducted in 880 mild AD patients receiving acetylcholinesterase inhibitors, but it was terminated due to a lack of Azeliragon efficacy. Multiple derivatives of Azeliragon with similar pharmacophores were developed that showed activity against RAGE-Aβ interactions through V domain binding, preventing Aβ transport across the BBB (Han et al., 2012, 2015; Y. S. Lee et al., 2012).

Another small molecule inhibitor of RAGE is N-Benzyl-N-cyclohexyl-4-chlorobenzamide (FPS-ZM1), discovered by Deane et al. through screening of 5000 compounds. The binding analysis of radiolabeled FPS-ZM1 demonstrated inhibitory constants with Aβ, S100B, and HMGB1 at 25, 230, and 148 nM, respectively (Deane et al., 2012). In in vivo studies in aged transgenic mice having mutations in the APP gene, the drug inhibited Aβ's BBB penetration, decreased RAGE expression, and improved cognitive function without significant toxicity. In a similar model of mice treated with a high level of AGEs, FPS-ZM1 administration reduced neuroinflammation and production of ROS (Y. Hong et al., 2016). Other studies demonstrated that FPS-ZM1 attenuated inflammation and improved cardiac remodeling following aortic ligation in C57BL/6 mice (Y. Liu et al., 2016). It also showed efficacy in breast cancer, reducing tumor growth, angiogenesis, macrophage invasion, and lung metastasis (Kwak et al., 2016).

3.2 | Peptide-derived antagonists

Another method in inhibiting RAGE activity is to utilize peptide sequences derived from ligands that directly bind to the receptor (Li et al., 2003). Huttunen et al. observed similarities in a positively-charged 33 amino acid sequence derived from HMGB1 and that of S100 proteins (Huttunen et al., 2002). They hypothesized that this peptide sequence could bind to RAGE and block RAGE-ligand activity. Although no binding kinetics were reported, it was shown that the 500 μM of the amino acid sequence inhibited 500 μM amphoterin-induced neurite outgrowth. The peptide suppressed in vivo pulmonary metastases of B16-F1 melanoma cells injected into immunocompromised mice. Further studies showed the peptide's ability to reduce inflammation in a BALB/C mouse model of acute lung injury (ALI) (S. Lee et al., 2018). Additionally, this peptide was utilized as a targeting system for the delivery of plasmid DNA (pDNA) therapy for ALI (Piao et al., 2019). The positive charge allowed it to complex with pDNA, and RAP targeted RAGE, which is overexpressed in the disease. This allowed for RAGE-mediated endocytosis into lung cells. In vivo studies of BALB/C mice showed this system possessed improved cell delivery and anti-inflammatory effects compared to polyethylamine (PEI)/pDNA complexes, a common gene therapy vehicle (Pandey & Sawant, 2016). Arumugam et al. developed a RAGE antagonistic peptide (RAP) from a sequence of S100P which inhibited binding against S100P, S100A4, and HMGB1 (Arumugam et al., 2012). This peptide reduced Nf-κB activity within pancreatic cancer xenografts of immunocompromised mice and attenuated tumor growth. In a BALB/C mouse model of asthma, blockage of RAGE by either RAP or FPS-ZM1 showed an equal effect in reduced inflammation and blunted airway activity, suggesting RAP as a potential therapy for RAGE-induced activity (Yao et al., 2016).

3.3 | Genetic therapies

Silencing of RAGE expression is an attractive route for therapy, as the reduction in RAGE expression can inhibit binding and signaling activity. Silencing RNA (siRNA) are short double-stranded RNAs that enter the cell and are incorporated into the RNA-Induced Silencing Complex (RISC), which targets and cleaves complementary messenger RNA (mRNA), inhibiting protein translation (Dana et al., 2017; Reynolds et al., 2004). Due to rapid degradation in vivo, siRNA therapies are complexed with polymeric carriers (Kanasty et al., 2013). Current RAGE siRNA therapies are complexed with PEI-based delivery vehicles (J. Hong et al., 2014; H. Park et al., 2015; M. J. Yang et al., 2015). Park et al. demonstrated the use of a deoxychloric acid-modified PEI (PEI-DA) carrier for RAGE siRNA to provide protection against cardiac arrhythmias in acute I/R injury (H. Park et al., 2015). Gene delivery restored electrophysiological properties that were disrupted in a LAD ligation/reperfusion model of Sprague–Dawley rats (J. Hong et al., 2014). PEFI-DA/RAGE siRNA complexes have also restored ventricular remodeling in MI rat models. Additionally, RAGE siRNA therapies have been shown to reduce inflammation-induced damage and ECM deposition in rat models of liver fibrosis (Cai et al., 2014; Xia et al., 2008).

3.4 | Antibody-drug conjugates (ADCs)

Monoclonal antibodies (mAbs), which target upregulated surface proteins, are a potential method to direct cytotoxic chemotherapies toward tumors (Sievers & Senter, 2013). Healey et al. developed RAGE mAbs conjugated to the chemotherapeutic monomethyl auristatin E (MMAE) that targeted the V, C1, and C2 domains (Healey, Pan-Castillo, et al., 2019). Surface plasmon resonance (SPR) demonstrated that V domain targeted ADCs possessed T H-score analysis from 161 biopsies showed increased RAGE expression in the stromal and epithelium cells of EC patients (Healey, Frostell, et al. 2019). RAGE ADC EC cells demonstrated high toxicity in EC cells and that toxicity was significantly reduced in healthy endometrium cells. Internalization and lysosomal trafficking analysis showed significantly higher ADC internalization in EC cells over controls, further demonstrating cell-specific targeting. Importantly, IV injection of ADCs and IHC analysis showed no signs of cytotoxicity within tissues of nude athymic mice. However, ADC treatment did reduce white blood cell counts. In a xenograft model of EC, ADC treatment showed reduced tumor volume (Healey, Frostell, et al. 2019). This study illustrates the potential for RAGE ADCs as a targeting agent.

3.5 | AGE crosslink breakers

Lysine-bound AGEs can undergo β-dehydration and react with ECM protein nucleophiles to form AGE crosslinks known as AP-enedioenes (Jud & Sourij, 2019; Vasan et al., 1996). These AGE crosslinks are associated with cardiovascular stiffness, oxidative stress, and inflammation (Brownlee, 2001; Yamagishi, 2012). Moreover, hyperglycemic conditions such as diabetes elevate AGE formation, increasing the formation of these crosslinks.

Crosslink breakers cleave carbon–carbon bonds, resulting in the reduction in both AGEs and their respective crosslinks. Alagebrium is an AGE crosslink breaker developed by Synvista Therepeutics (formerly Alteon) that has shown efficacy in both preclinical and clinical cardiac disorders (Toprak & Yigitaslan, 2019; Yamagishi, 2012). Within streptozotocin-induced diabetic rats, Alagebrium treatments significantly reduced large artery stiffness and collagen crosslink formation (Wolffenbuttel et al., 1998). It was also shown that AGE modified serum albumin negatively affected vasodilation within nondiabetic rats; it was found that the endothelial nitric oxide synthase (eNOS) was upregulated and Alagebrium administration attenuated these effects (Soro-Paavonen et al., 2010). Within atherosclerotic and diabetic ApoE-negative mice treated with early and delayed Alagebrium exhibited reduced RAGE expression, proinflammatory cytokines, arterial plaque area, and circulating AGEs (Forbes et al., 2004; Watson et al., 2011). A 13-person clinical trial involving elderly men with systolic hypertension showed that Alagebrium reduced arterial stiffness, and a flow mediated dilatation was inversely related to collagen synthesis and inflammation markers (Zieman et al., 2007). In a 26-person clinical trial, elderly patients with stable diastolic heart failure (DHF) were treated with 400 mg/day Alagebrium. Both magnetic resonance imaging (MRI) and echocardiology analysis revealed a reduction in left ventricular mass and increase in diastolic filling (Little et al., 2005). A double-blind trial with 102 elderly patients with systolic heart failure, 200 mg/day failed to attenuate skin AGE accumulation and improve cardiac function (Hartog et al., 2011). In addition to cardiology, Alagebrium has been utilized for nephrologic diseases. AGE administration induced an epithelial-to-myoblast transition within both diabetic rats and T1D patient biopsies; Alagebrium mitigated this effect (Oldfield et al., 2001). Treatment of T2D mice with a high-AGE diet showed improved renal clearance of creatine (Harcourt et al., 2011). Alagebrium has also demonstrated efficacy within pancreatic β-islet destruction, chronic kidney disease-mineral bone disorder age-related macular degeneration (N. X. Chen et al., 2020; Coughlan et al., 2011; Datta et al., 2008). In addition to Alagebrium, other AGE crosslink breakers have been developed. For example, 3–2-(methylsulfoxyl) hydrazine carbonyl-1-2-oxo-2-2-thienyl ethyl-chloride (TRC4186) improved cardiac and renal dysfunction with T2D hypertensive fatty rats (Joshi et al., 2009). TRC4186 was also well tolerated in a Phase I clinical trials (K. P. Chandra et al., 2009). Other representative of AGE crosslink breakers, 3-benzyloxycarbonylmethyl-4-methyl-thiazol-3-ium bromide (C36) has also shown promise as an AGE breaker in improving arterial compliance of diabetic rats (Cheng et al., 2007).

In conclusion, AGE crosslink breakers hold promise as a potential therapeutic strategy for age-related diseases characterized by the accumulation of AGEs. These compounds have been shown to reduce tissue stiffness, improve vascular function, and alleviate inflammation in preclinical studies. However, further research is needed to establish their safety and efficacy in human trials. Moreover, as the underlying mechanisms of AGE-mediated pathologies are complex, it is likely that a multi-faceted approach targeting both AGE formation and scavenging and AGE crosslinking will be necessary for effective treatment of age-related diseases.

3.6 | Soluble RAGE

Soluble RAGE (sRAGE) acts as a scavenger of RAGE ligands, and it has shown therapeutic potential via exogenous administration. This is highlighted in multiple diabetic inflammatory complications, as RAGE overexpression drives chronic inflammation. In a study by Wendt et. al, ApoE mice treated with sRAGE for 8 weeks showed a reduction in atherosclerotic lesions and proinflammatory and thrombotic gene expression within aortas (Venegas-Pino et al., 2018). In genetically diabetic C57BLKS/J-m+/+Leprdb mice, skin wounds topically treated with sRAGE possessed improved wound closure and neovascularization. Interestingly, sRAGE treated mice showed a higher level of inflammatory cell infiltrate during the first 35 days which then decreased. Within control groups, inflammatory cell and pro-inflammatory cytokine levels were sustained following 35 days, leading to a failure of remodeling and wound closure. Additionally, endogenous elevation through genetic modification of cells are another method of sRAGE delivery. Park et al. developed sRAGE overexpressing adipose-derived mesenchymal stem cells (MSCs) which were intravenously administered

to BALB/C mice receiving collagen-induced arthritis (M.-J. Park et al., 2016). sRAGE-MSCs inhibited the expression of HMBG1 pro-inflammatory cytokines in both MSCs and joints. These areas also exhibited greater T-regulatory cell infiltration and Th17 cell reduction, indicating the joint microenvironment is anti-inflammatory.

A similar strategy was applied to a PD mouse model using CRISPR-Cas9 edited MSCs. These treatments showed reduced neuronal death and inhibited AGE localization with microglial cells, suggesting that one means for sRAGEs neuroprotective effects may be through scavenged AGEs. While sRAGE has shown potential, sRAGE ligands bind to additional receptors such TLRs and CD36, and the effects of their inhibition need to be determined. There is some evidence to suggest sRAGE administration can lead to negative outcomes. In sciatic nerve injury, administration of sRAGE blocked nerve regeneration due to the inability to trigger inflammatory mechanisms which cause nerve outgrowth. Thus, it is important to further understand the complex role sRAGE exhibits in pathology to better utilize it in therapeutic applications.

3.7 | Dietary intervention

Another interesting but still underexplored strategy to suppress RAGE activity to prevent RAGE/AGE axis associated pathologies is the modification of the diet to reduce AGEs intake. Approximately about 10% of consumed AGEs are absorbed through the intestines. About one-third of absorbed AGEs are excreted within 48 h in the urine. In contrast, the rest remain in the tissues fueling the inflammation and contributing to the deleterious effects of RAGE overexpression (Diamanti-Kandarakis et al., 2015). Dietary restriction of the consumption of AGEs from exogenous sources through modification of eating habits is now considered an initial, effective therapeutic intervention in managing several AGE-related disorders. While dietary restriction and the use of a low AGE diet have been shown beneficial to improve insulin sensitivity, reduce abdominal obesity, diminish oxidant stress and extend lifespan (Garay-Sevilla et al., 2016), further research is needed to establish the safety and efficacy of dietary interventions in clinical trials.

4 | IMAGING RAGE WITH MOLECULARLY TARGETED AGENTS

4.1 | Preclinical and clinical imaging modalities

Molecular imaging is a field of medical imaging that uses specialized imaging techniques to visualize and study the molecular and cellular processes within the body. This type of imaging provides a way to understand the underlying biology of disease, and can be used to detect, diagnose, and monitor the progression of a wide range of conditions. One of the main strengths of molecular imaging is its ability to provide detailed information about the molecular and cellular processes that are involved in disease. This can be particularly useful in the early detection of cancer, as well as in the monitoring of treatment response. In addition, molecular imaging can be used to evaluate the effectiveness of new drugs and therapies, which can help to improve patient outcomes.

However, there are also some limitations to molecular imaging. One of the main challenges is the high cost of the imaging equipment and the specialized expertise required to operate and interpret the images. Additionally, the images generated by molecular imaging techniques can be complex and difficult to interpret, which can make it challenging for physicians to use the information to guide patient care. Overall, molecular imaging is a powerful tool for understanding the underlying biology of disease, and has the potential to improve patient outcomes. However, further research and development is needed to overcome the limitations of this technology and make it more widely available to patients.

A comprehensive examination of the current pre- and clinical uses of molecular imaging and the associated challenges has helped to identify potential areas for future growth in this field. These include: exploring the mechanism of biological processes in vivo, evaluating the metabolism and pharmacology of new therapeutic interventions, and enabling their rapid introduction into clinical practice. However, for this process to be successful, there is a current need for new technology platforms, such as integrated microfluidic methodologies to speed up and reduce the cost of developing and testing new molecular imaging probes. In addition, there is a need for higher-resolution, higher-sensitivity imaging instruments to detect and quantify biological processes more efficiently and accurately. Despite the exciting possibilities of improving patient care through the translation of preclinical imaging approaches, the decline in infrastructure, loss of federal research support, and prolonged, ineffective approval processes for new imaging probes

pose significant threats to the advancement of molecular imaging. Addressing these challenges through strategic planning is critical for rejuvenating the field and realizing its full potential.

Over the past 40 years, numerous imaging modalities have been introduced, but only a few have found widespread use of both preclinical and clinical research. These include nuclear imaging techniques such as positron emission tomography (PET), single photon emission computed tomography (SPECT), magnetic resonance imaging (MRI), ultrasound, as well as x-ray computed tomography (CT) and optical imaging such as fluorescence (Table 1). The best imaging method choice for a particular study depends on the availability of both the instrumentation and imaging probe(s), and the priority of desired features. For example, anatomical imaging modalities such as CT, ultrasound and MRI are optimal for imaging anatomy and physiology, whereas functional modalities such as nuclear imaging and optical techniques are superior to assess metabolic and molecular processes (Figure 2). A comprehensive evaluation of each imaging modality, including its strengths and weaknesses, is beyond the scope of this manuscript. For more information, readers are referred to relevant reviews (Bengel, 2009; Lawrence W. Dobrucki & Sinusas, 2010; Nahrendorf et al., 2009; Sinusas et al., 2008; Vaquero & Kinahan, 2015; Walter et al., 2020).

Nuclear imaging, including PET and SPECT, belong to clinical imaging modalities which have been proven successful in quantifying radiotracer uptake and distribution due to their excellent sensitivity, good temporal resolution and reasonable spatial resolution, particularly in the new preclinical scanners (Basu et al., 2011). PET imaging is advantageous when considering its superior sensitivity, practically limitless penetration depth, and the ability for a high temporal resolution dynamic imaging (dPET) which can provide useful information to assess pharmacokinetic parameters derived from, that is, compartmental computational modeling of radiotracer's fate (Vaquero & Kinahan, 2015).

The labeling of PET pharmaceuticals can be challenging considering the short half-life of traditional PET radioisotopes such as Carbon-11, Nitrogen-13, or Oxygen-15, which requires the presence of on-site production cyclotron or generator. Among clinically available radioisotopes, only Fluorine-18 has an adequate half-life (~2 h) that allows for off-site production and delivery via courier. Other radioisotopes such as Copper-64 (12.7 h half-life) and Zirconium-89 (3.3 days half-life) are currently evaluated in preclinical models with the promise to be translated to clinical use (De Silva et al., 2012; Wadas et al., 2007; Zeng et al., 2012).

A historically older nuclear imaging technique, SPECT, is based on the detection of gamma radiation emitted from an unstable atomic nucleus. SPECT radioisotopes are characterized by their relatively longer (as compared to PET)

TABLE 1 Selected operational parameters including advantages and disadvantages of different molecular imaging modalities.

Imaging modality	Sensitivity	Spatial resolution	Temporal resolution	Major advantages	Major disadvantages
PET	Picomolar	>0.35 mm	Seconds	Superior sensitivity Good attenuation correction	Short half-life radioisotopes Require on-site generation
SPECT	Nanomolar	>0.25 mm	Minutes	Great sensitivity Multiple isotope imaging	Exposure to ionizing radiation Advanced radiochemistry
MRI	Micromolar	>0.50 mm	Seconds	No ionizing radiation Great spatial resolution	Limited sensitivity Susceptible to motion artifacts
X-ray CT	Millimolar	μm–mm	Milliseconds	Superior spatial resolution Availability of contrast agents	Exposure to ionizing radiation Contrast agent nephrotoxicity
Fluorescence	Picomolar	nm–mm	Seconds	Superior sensitivity Multiplexing imaging possible	Prolonged exposure bleaching Fluorescent labels required
Ultrasound	Micromolar	μm–mm	Seconds	Widely available instrumentation No ionizing radiation	Limited penetration depth Lack of molecular probes

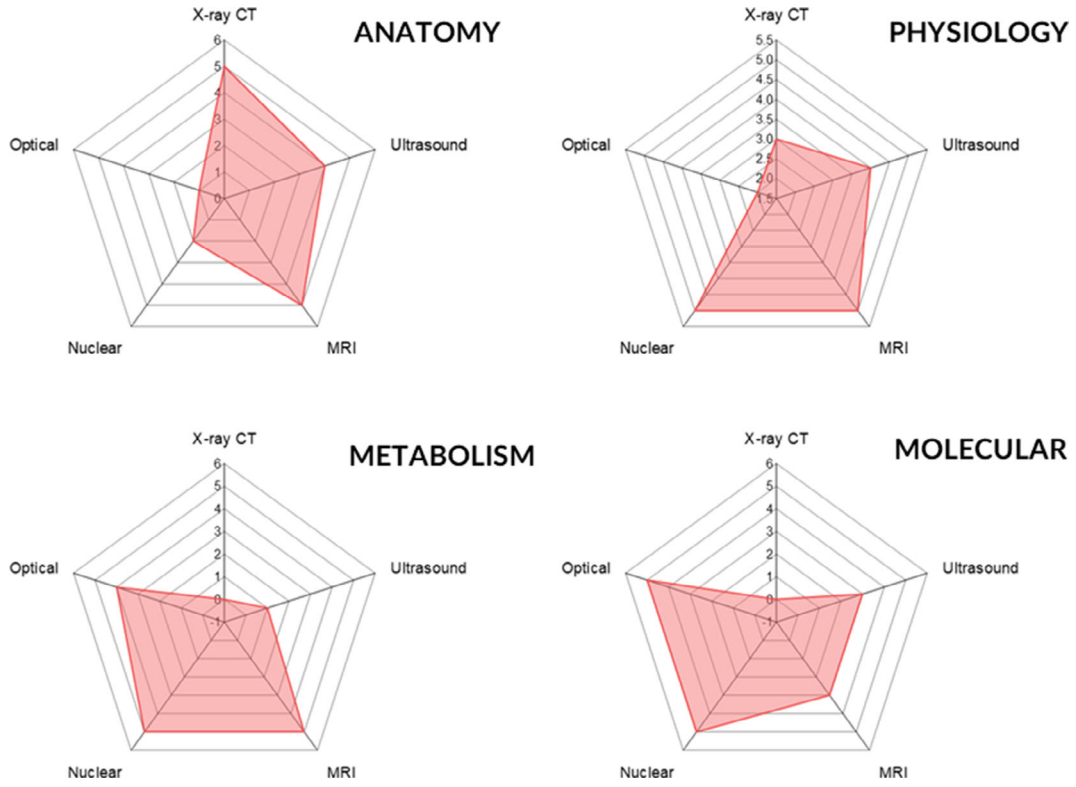

FIGURE 2 Comparison of selected clinical imaging modalities for assessing anatomy, physiology, metabolism, and molecular processes. A spider chart for each feature illustrates the suitability of each imaging modality using a scale of 1–5, with "1" indicating low and "5" indicating high applicability.

half-lives (hours to days) which allow for longitudinal imaging studies and have specific emission spectra which allow for simultaneous multiple isotope imaging (Mariani et al., 2010). One important disadvantage of SPECT shared also with PET, is the use of ionizing radiation which can limit their application to specific cases where exposure to the ionizing radiation is acceptable considering the benefits of noninvasive imaging of molecular processes. Also, since different radioisotopes have different physicochemical properties, radiolabeling of molecules or bioactive targets requires access to the radiochemistry resources and the knowledge of traditional conjugation chemistry. Finally, radiolabeling with SPECT isotopes, often requires chelation which can increase the molecular weight of the target molecule, may change the overall charge, and cause steric hindrances affecting pharmacokinetic properties of the radiotracer. In contrast, PET radioisotopes such as Carbon-11, Nitrogen-13, and Oxygen-15 can be incorporated in the molecule with minimal interference to the function of the tracer. This feature allows for developing radiolabeled probes, which are chemically almost identical to the parent compounds. This strategy has been successfully employed to develop PET tracers which can pass the blood–brain–barrier (BBB) and be taken up by brain structures to assess their function (Judenhofer & Cherry, 2013; Mariani et al., 2010).

In optical imaging, such as fluorescence, light originates from light-excited tissues containing fluorescent label(s). The emitted light is captured by a charge-coupled device (CCD) camera and recorded for processing. Fluorescent molecules like cyanine dyes (i.e., Cy3 or Cy5), are commonly used to label bioactive targets and trace their biodistribution in the biological system. The alternative method involves transfecting cells with a gene, such as green fluorescent protein (GFP), to study cell function and survival. Fluorescence imaging has several advantages, including ease of use, high throughput, relatively low cost, and no ionizing radiation. However, its clinical use is limited by reduced depth penetration, surface reflectance, hemoglobin absorption, scattering, and background autofluorescence. These drawbacks have effectively ruled out optical techniques for clinical whole-body imaging, limiting their use to only local examinations, such as image-guided surgery or postmortem tissue analysis (J. H. Lee et al., 2012).

In recent decades, research has been focused on developing and characterizing molecularly targeted imaging agents for in vivo analysis of biological processes at the cellular, organ, and whole-body levels. The molecular imaging of RAGE expression and its activation using both nuclear and optical imaging techniques hybridized with anatomical

imaging modalities has been proven successful in evaluating the significance and quantitatively assessing the function of the RAGE/AGE axis in vivo. The critical review of the most impactful studies focused on imaging RAGE and utilizing antibody fragments, peptides, small chemicals, and targeted nanoparticles is presented in the following sections.

4.2 | Antibodies and antibody fragments

Antibodies and antibody fragments have become essential components in the field of molecular imaging. With their high specificity and ability to selectively bind to target proteins, they provide a valuable tool for visualizing biological processes in real-time. By conjugating these molecules with imaging agents, researchers can obtain detailed information about the distribution and localization of target proteins within living organisms, including both healthy and diseased tissues. In this way, antibodies and antibody fragments play a critical role in advancing our understanding of biological processes, informing the diagnosis and treatment of diseases, and improving patient outcomes. The use of antibodies and antibody fragments in molecular imaging is therefore a rapidly growing field with great potential for contributing to the development of new diagnostic and therapeutic strategies.

Early molecular imaging involved native monoclonal antibodies labeled with signals, which provided high sensitivity and selectivity. However, long circulation times of antibodies and their slow excretion resulted in poor image quality and strong background signals which could mask specific organ uptake (L. W. Dobrucki et al., 2010). To address this limitation, tracers based on engineered antibodies and antibody fragments were developed for imaging cell-specific antigens, including RAGE.

The first successful synthesis of radiolabeled anti-RAGE antibody fragment and its application in preclinical imaging was reported by Lynne Johnson group at Columbia University (Y. Tekabe et al., 2008). The authors of this pilot study developed a novel antibody based on the Genbank sequence which displayed immunoreactivity against the V-domain of RAGE in mice, pigs and humans. The purified antibodies were digested with immobilized pepsin beads to produce $F(ab')_2$ fragments. In contrast to the whole antibody, these fragments had more antigen binding sites available and demonstrated faster blood pool and renal clearance. Radiolabeling with Technetium-99 m (^{99m}Tc) was performed after coupling $F(ab')_2$ fragments to diethylenetriaminepentaacetic acid (DTPA). In addition to the radiolabeled anti-RAGE antibody fragments for the in vivo planar imaging, the investigators prepared a rhodamine-labeled DTPA-anti-RAGE $F(ab')_2$ analogue which has been used to localize the in vivo antibody uptake by histology. The antibody-based tracer showed a rapid blood clearance and specific focal uptake in the aortic arch of atherosclerotic apoE−/− mice correlating with atherosclerotic lesions seen during the necropsy. This specific uptake was quantified by ex vivo counting of thoracic organs such as lungs, heart and aorta. Histological sections through the proximal aorta of apoE −/− mice injected with dual rhodamine and ^{99m}Tc labeled $F(ab')_2$ showed colocalization of fluorescence with RAGE staining. This confirmed that the dual-labeled antibody fragments were taken up in the proximal aortic lesions expressing RAGE (Y. Tekabe et al., 2008).

The same group extended this work and developed ^{99m}Tc-labeled monoclonal anti-RAGE antibody demonstrating improved specificity compared to the polyclonal antibody (Yared Tekabe et al., 2010; Y. Tekabe et al., 2010). This monoclonal antibody-based imaging agent demonstrated that RAGE-targeted molecular imaging can detect the effect of diabetes on RAGE expression in a diabetic murine model of hindlimb ischemia (Yared Tekabe et al., 2013). In this study, C57BL/6 mice were rendered diabetic and 2 months later subjected to the surgical ligation of left femoral artery to induce peripheral ischemia. Five days later, both diabetic and nondiabetic control animals were injected with a monoclonal ^{99m}Tc-anti-RAGE $F(ab')_2$ tracer and imaged 5 hrs later with a preclinical SPECT-CT scanner (Figure 3). Authors have demonstrated higher quantitative uptake of RAGE-targeted probe in the nonischemic limbs of the diabetic compared to the nondiabetic nonischemic limbs, which supports that diabetes alone could induce RAGE expression in the peripheral arteries. Furthermore, the uptake of the probe on coronal slices from SPECT/CT scans following injection of ^{99m}Tc-anti-RAGE $F(ab')_2$ at 5 days after left femoral artery ligation showed greater uptake of the tracer in the ischemic limbs of diabetic mice compared to the probe uptake in the ischemic limbs of nondiabetic mice or in the ischemic limb of mice injected with nonspecific IgG $F(ab')_2$ (control probe).

Following the early success in imaging RAGE using radiolabeled F(ab')2 antibody fragments in small animals, more recent paper by Tekabe et al demonstrated, using the previously synthesized radiolabeled antibody, enhanced RAGE expression in coronary and carotid fibroatheromas and in the small arteries of large animal's hindlimbs (Johnson et al., 2014). Although studies in atherosclerosis and peripheral arterial disease confirm that RAGE overexpression can be successfully used as a target for molecular imaging, it has not been extensively evaluated in a

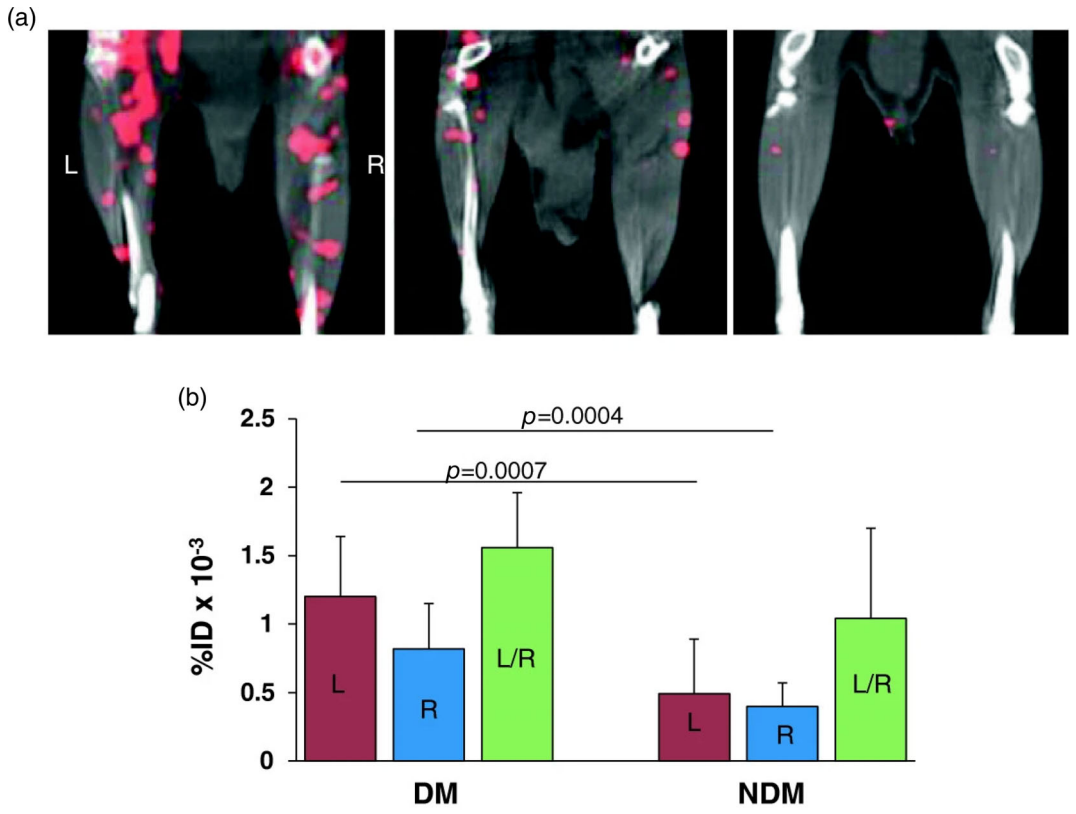

FIGURE 3 (a) Representative coronal slices from SPECT/CT scans following injection of 99mTc-anti-RAGE F(ab')2 5 days after left FAL for a WT diabetic mouse (left), WT nondiabetic mouse (center), and WT nondiabetic mouse injected with nonspecific mouse IgG $F(ab')_2$ (right). (b) A bar graph shows quantitative RAGE uptake from scans in hind limbs for WT diabetic (left set of bars) and WT nondiabetic (right side set of bars) 5 days after FAL. Each bar represents average ± SD. DM, diabetes mellitus; NDM, nondiabetes mellitus; FAL, femoral artery ligation; WT, wild type. Reproduced with permission from Tekabe et al. (2013).

nondiabetic milieu. In this study, hyperlipidemic pigs were injected with 99mTc-anti-RAGE F(ab')2 and after 6 h blood clearance subjected to SPECT-CT imaging of neck, thorax and hind limbs. For experimental control, a subset of hyperlipidemic pigs was injected with a nonimmune IgG $F(ab')_2$ and several farm pigs were injected with RAGE-targeted tracer. Following image analysis, it was evident that the focal vascular uptake of the targeted tracer visualized on SPECT scans corresponded to class III/IV lesions in the coronary and carotid vessels. In addition, uptake in the hind limbs was noted in the hyperlipidemic pigs and corresponded to RAGE staining of small arteries in the muscle sections (Figure 4).

The same group of investigators took on the task to image expression of RAGE in a mouse model of myocardial reperfusion injury (Y. Tekabe et al., 2012). They hypothesized that RAGE-directed quantitative imaging of myocardial uptake of ^{99m}Tc-anti-RAGE $F(ab')_2$ in a mouse model of myocardial ischemic injury can detect RAGE expression and show quantitative differences between early (18–20 h) and later times (48 h) after reperfusion. The results of this study demonstrated that RAGE expression in the myocardium subjected to ischemia/reperfusion injury can be imaged and quantified in live animals with a radiolabeled anti-RAGE antibody and SPECT imaging. Immunohistology showed colocalized RAGE expression primarily to cardiomyocytes and activation of apoptotic pathways (caspase staining).

Although the feasibility of molecular imaging of RAGE with the antibody-based RAGE-targeted tracer has been successfully demonstrated in several animal models, this strategy is not without limitations. The long residence time of antibody-based imaging agents in the bloodstream results in high background and lower quality images. Furthermore, these imaging agents have limitations in terms of being single modality tracers, lacking drug payload capability, and poor optimization for the number of binding ligands and reporter molecules.

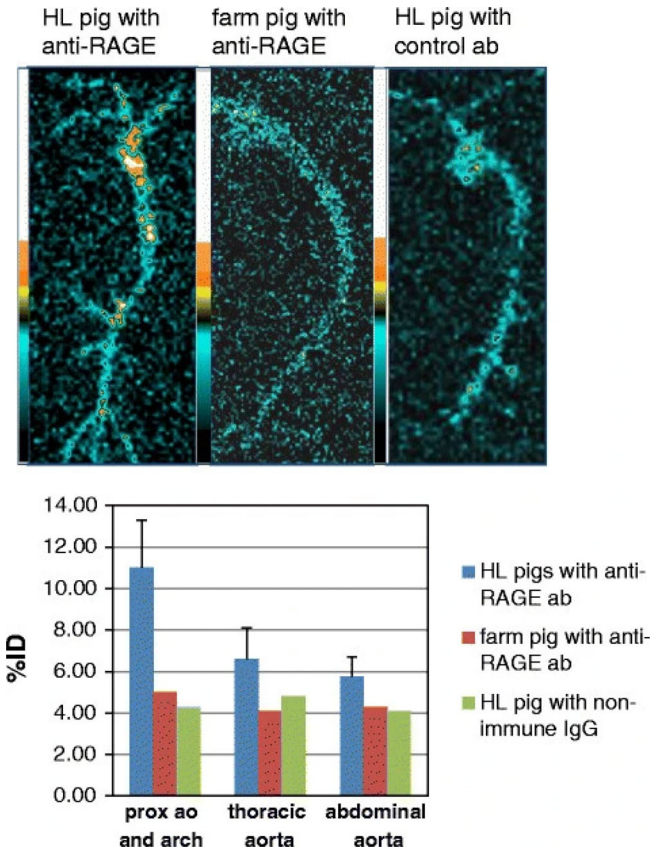

FIGURE 4 Ex vivo imaging of RAGE in the pig's aorta. The top-row images are the planar scans of the aortas from an HL pig injected with ^{99m}Tc-anti-RAGE F(ab')$_2$ (left), a farm pig injected with the same antibody in the middle, and an HL pig injected with radiolabeled control antibody on the right. Tracer uptake is seen in the distal arch and proximal thoracic aorta in the HL pig, but no appreciable focal uptake is seen on the aortas from the farm pig and the HL pig injected with the control antibody. The graph below shows uptake as %ID, with blue bar representing the mean ± SD for all the HL pigs injected with ^{99m}Tc-anti-RAGE F(ab')$_2$ and average values for three farm pigs and two HL injected with nonimmune IgG. The small increment of uptake of ^{99m}Tc-anti-RAGE F(ab')$_2$ over the controls corresponded with low expression on histology. Reproduced with permission from Johnson et al. (2014).

4.3 | Peptides and peptidomimetics

Peptides and peptidomimetics have revolutionized the field of molecular imaging, offering a powerful tool to visualize biological processes in real-time. With their high specificity and ability to target specific proteins or cells, they provide a window into the inner workings of the body, providing critical information for the diagnosis and treatment of disease. Whether used for imaging the progression of cancer, tracking the delivery of drugs, or visualizing the activity of the immune system, peptides and peptidomimetics are a versatile tool for advancing our understanding of human biology and improving patient outcomes.

There are only a limited number of published studies that utilize peptides and peptidomimetics for molecular imaging of the RAGE. The scarcity of research in this area can be attributed to several factors. First, RAGE is a relatively new target, and its expression has only recently been discovered in several pathologies, including cancer, cardiovascular, and neurodegenerative diseases. Hence, the identification of targeted peptides and development of peptidomimetics as imaging probes targeting RAGE is still in its early stages. Second, the development of RAGE-targeting imaging probes based on targeted peptides is challenging by the limited understanding of the receptor's structure and binding sites. RAGE has several domains, and its ligands can bind to different regions, making it difficult to identify the most effective target site for imaging probes.

Despite these challenges, some promising studies have shown that peptides and peptidomimetics can be used as imaging probes for RAGE. For instance, a recent study by Dobrucki group at the University of Illinois at Urbana-Champaign demonstrated that a decapeptide targeting the V domain of RAGE could be used for imaging of RAGE

expression in a mouse model of breast cancer. As the backbone of this tracer, the authors used RAGE antagonistic peptide (RAP) which was found to prevent RAGE from binding with several of its most essential ligands (Arumugam et al., 2012). In this study, multimodal probes targeting RAGE were synthesized using the standard solid-phase peptide synthesis method and labeled with FITC and Cy7 fluorophores or radiolabeled with Copper-64 (^{64}Cu). Their stability was tested in PBS and rat plasma with RP-HPLC and cellular binding properties were determined in 4T1 breast cancer cells using flow cytometry and radiological methods. To evaluate in vivo pharmacokinetics, tumor binding, and organ biodistribution, RAGE-targeted probes were injected intravenously into 4T1 xenograft-bearing mice for dynamic PET-CT imaging followed by fluorescence imaging and postmortem gamma well-counting. To evaluate nonspecific binding, an excess of unlabeled RAP was used for in vivo blocking and competition experiments. Finally, excised 4T1 tumors were collected and processed for immunohistochemical staining. The probes' stability was found to be high during the first 4 hours of incubation in plasma and PBS. Flow cytometry data confirmed probes' specificity, sensitivity, and selectivity to RAGE-positive 4T1 cancer cells. In vivo, dynamic PET-CT imaging demonstrated rapid blood clearance and a predominant kidney-urine elimination route. Competition experiments showed a 63% reduction of RAGE-targeted probe signal due to significant blocking of RAGE with RAP excess. Finally, the correlative PET-optical imaging, supplemented with gamma well-counting data, demonstrated the focal uptake of RAGE-targeted tracers in the tumor and its microenvironment, with activities detected in the liver, kidneys, and lungs (Figure 5). The new class of RAP-based multimodal probes demonstrated great promise for targeting RAGE-positive tissues and microenvironments with high specificity, sensitivity, and selectivity. The nuclear imaging with a radiolabeled probe showed favorable biodistribution, rapid blood clearance, and a preferable excretion route for potential clinical translation of this technology. In addition, the availability of optical RAGE-targeted analogues can provide correlative capabilities for targeting and imaging RAGE-positive tissues in vitro, in vivo, and postmortem.

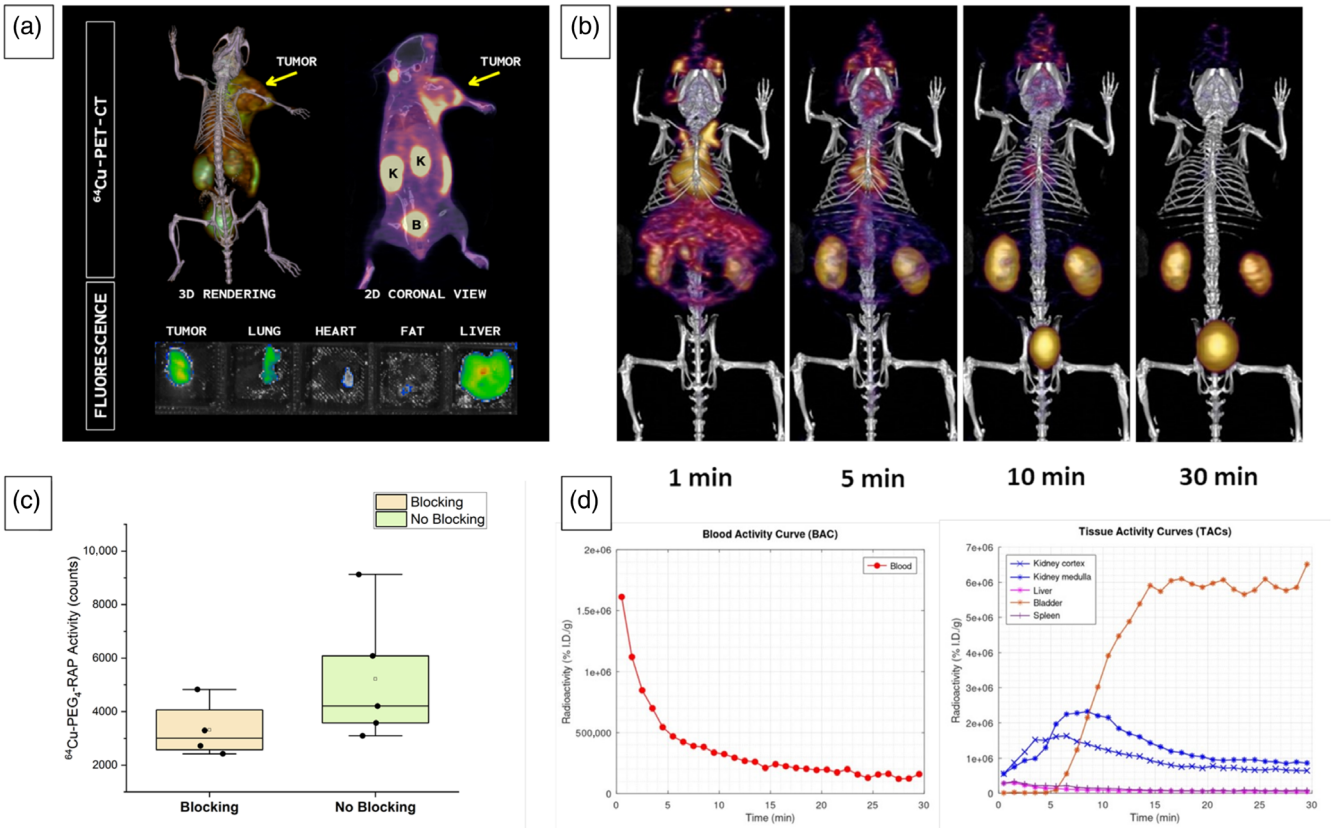

FIGURE 5 Representative in vivo whole-body PET-CT and postmortem organ fluorescence imaging of RAGE in a mouse bearing 4T1 murine breast cancer xenograft. Animals were imaged with multimodal RAGE antagonistic peptide (RAP) based molecularly targeted ^{64}Cu-NOTA-PEG$_4$-RAP and Cy7-PEG$_4$-RAP probes. These tracers demonstrated focal (a) and specific (c) uptake within the tumor and its microenvironment, liver, and spleen and predominant elimination via kidney filtration and urine collection in the bladder. Dynamic PET (b) showed rapid blood clearance and preferable pharmacokinetics (d). Illustration provided by courtesy of Dr. Lawrence W. Dobrucki.

Despite this early success in developing peptide-based RAGE-targeted imaging probes and demonstrating their potential applicability in imaging pathologies associated with dysregulated RAGE, the limited number of published studies on peptides and peptidomimetics for molecular imaging of RAGE can be attributed to the challenges associated with developing imaging probes for this complex receptor. However, with advances in understanding the structure and binding sites of RAGE and the development of novel imaging technologies, it is expected that more studies will emerge in this area.

4.4 | RAGE-targeted small molecules

Small molecules are frequently used as probes for molecular imaging. In contrast to other imaging strategies, such as antibody-, peptide-, or nanoparticle-based agents, small molecules are characterized by a combination of high sensitivity, low toxicity and easy synthesis. Small molecules can be designed to target specific biological processes or molecular structures (e.g., as receptor antagonists), providing high specificity for molecular imaging (Yi et al., 2022). They are also generally well-tolerated by the body and have low toxicity, making them safe for use in vivo which can also aid in their rapid clinical translation. Finally, small molecules are typically easy to synthesize in large quantities, and their synthesis can be relatively easy automated allowing for widespread availability and use in molecular imaging.

A number of small-molecule mediators of RAGE interactions have been reported (Deane et al., 2012; Han et al., 2012, 2014). In the study published by Cary et al., authors synthesized and evaluated a novel Fluorine-18 (^{18}F) labeled small molecule for PET imaging of RAGE in the brain (Cary et al., 2016). As a backbone, they used *N*-Benzyl-4--chloro-*N*-cyclohexylbenzamide (FPS-ZM1) which is a multimodal RAGE-specific inhibitor with a high (25 nM) affinity against RAGE, lack of toxicity in mice or cells, high specificity and BBB permeability allowing for imaging of RAGE-associated neurological disorders such as AD. In their work, the authors reported the synthesis and preliminary preclinical evaluation of ^{18}F-RAGER: a PET probe based on FPS-ZM1 and the first BBB-penetrative small molecule radiotracer for RAGE (Cary et al., 2016; L. R. Drake et al., 2020).

^{18}F-RAGER autoradiography showed colocalization with RAGE identified by immunohistochemistry in AD brain samples, and ^{18}F-RAGER microPET confirmed CNS penetration and increased uptake in areas of the brain known to express RAGE (Figure 6). This first-generation radiotracer serves as an initial proof-of-concept and a promising starting point for quantifying cerebral RAGE activity using PET. However, high levels of nonspecific ^{18}F-RAGER binding were observed in vitro, likely due to its high logP, and rapid metabolism in rat liver microsome studies. An estimated binding potential (BP) of ^{18}F-RAGER in AD tissue is 1.86, indicating potential suitability for future clinical PET imaging of RAGE but leaving room for improvement. Therefore, the development of second-generation radiotracers with Kd $\leq$6 nM is necessary to achieve the target BP of $\geq$5) for successful in vivo clinical imaging of RAGE in the future (as recommended by the National Institutes of Health for CNS radiotracers). To address these needs, ongoing efforts to improve affinity, reduce lipophilicity to minimize nonspecific binding, and rapid metabolism of the tracer are centered around developing new radioligands based on the FPS-ZM1 scaffold (Cary et al., 2016; L. Drake & Scott, 2018).

4.5 | RAGE-targeted nanoparticles

Many of the previously described RAGE-targeted probes, including antibody-, peptide-, and small chemical-based tracers, despite their proven use in many applications, suffer from several limitations associated with probes' chemical structures, including not-ideal pharmacokinetics properties. For example, probes utilizing RAGE antibodies or RAGE antibody fragments are known for characteristically long blood residence times, resulting in high background and lower quality images. In addition, these tracers are practically limited to only a single imaging modality reducing their applicability in multimodal imaging applications. Finally, due to their distinct chemical structures, these RAGE-targeted probes often have no drug payload capabilities which limit their use in theranostics applications, where organ-specific targeting and targeted drug delivery are imaged at the same time.

To overcome the limitations of using antibodies, peptides, or small chemicals in designing of molecularly targeted imaging probes, researchers sought nanotechnology, which allows for development of a multimodal multifunctional nanoparticles for future personalized medicine applications. Nanoparticles have been widely explored as vehicles for targeted drug delivery due to improved efficacy and reduced side effects. Compared to conventional drugs, nanoparticle formulations can be tuned for the delivery of a therapeutic cargo. Functionalization of nanoparticle constructs could

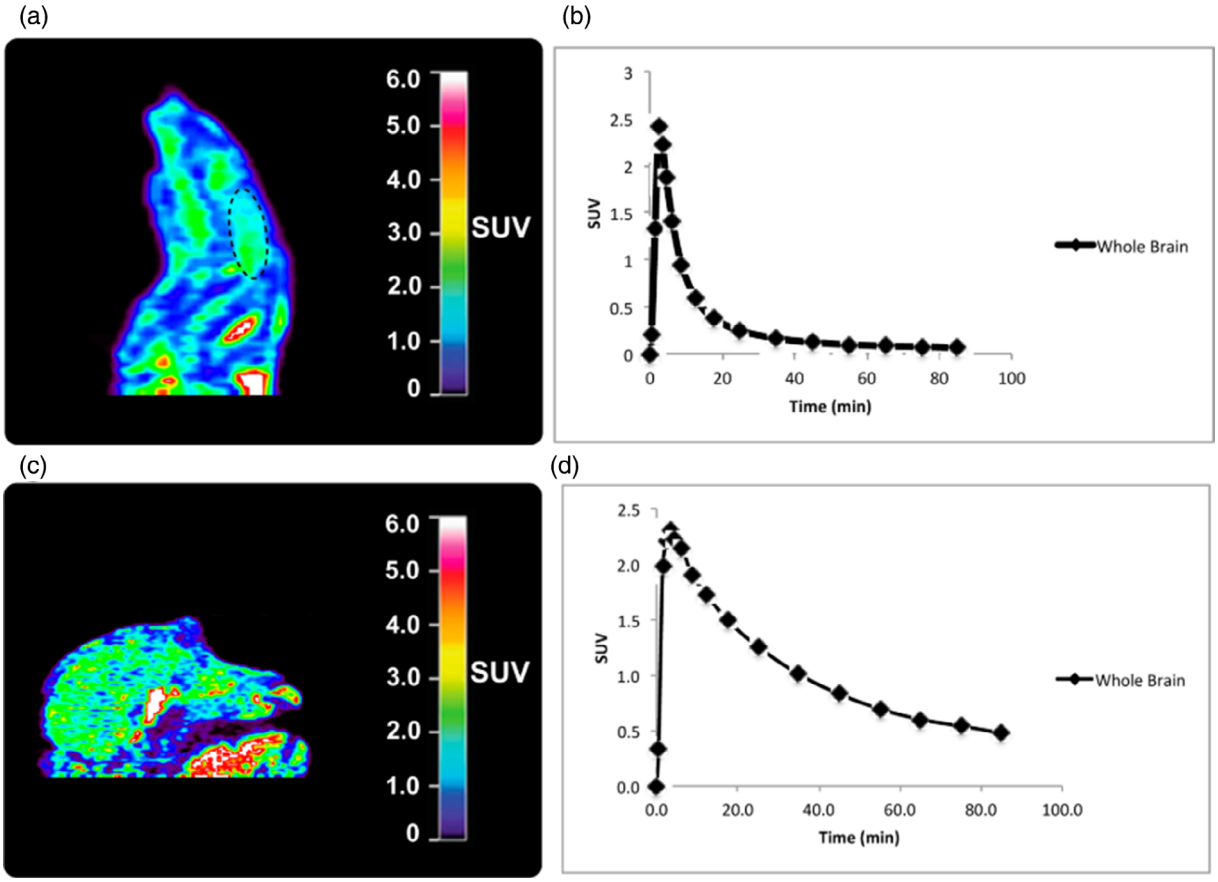

FIGURE 6 Representative microPET imaging data for rodent (a) summed images 0–90 min post-iv injection of the radiotracer (dotted oval = brain); (b) rodent whole brain time-radioactivity curves and nonhuman primate (c) summed images 0–90 min post-iv injection of the radiotracer; (d) nonhuman primate whole brain time-radioactivity curves imaged with ^{18}F-RAGER. Reproduced with permission from Cary et al. (2016).

also optimize probe's physicochemical properties, render them multimodal, and selectively target specific organs or tissues by conjugation of molecular ligands such as antibodies, aptamers, peptides, peptidomimetics, and small molecules (Lawrence W. Dobrucki et al., 2015). Despite these clear advantages, nanoparticles, especially these used in imaging applications, have typically long blood residence circulation increasing background signals and are significantly retained by liver and spleen, limiting their application to image these organs. Additionally, it has been estimated that less than 1% of injected dose reaches a target after systemic administration, reducing imaging sensitivity and therapeutic effect (Lawrence W. Dobrucki et al., 2015).

Recent developments in nanomedicine led to the design and chemical and biological characterization of multifunctional nanocarrier platforms which include multimodal molecularly targeted constructs based on polymers, dendrimers, liposomes, micelles, solid lipid and metal nanoparticles. One such platform used to develop targeted nanoparticles for imaging applications is poly(amidoamine) (PAMAM) dendrimers. PAMAM dendrimers' peripheral amine groups can be functionalized with targeting moieties and labeled with radioisotopes or fluorophores rendering them useful in various diagnostic and therapeutic biomedical applications (Labieniec-Watala & Watala, 2015).

Molecularly targeted nanoparticle for multimodal and multiscale imaging of RAGE in preclinical disease models was first synthesized and characterized in vitro and in vivo by Konopka et al. (2018). RAGE-targeted ^{64}Cu-Rho-G_4-CML nanoparticle was based on a generation 4 (G_4) PAMAM dendrimer, labeled with PET radioisotope (Copper-64, ^{64}Cu) and optical fluorophore—rhodamine, and rendered specific for RAGE by conjugation of a well-characterized RAGE ligand, carboxymethyl-lysine (CML)-modified human serum albumin (HSA) via a succinimidyl-(*N*-methyl-polyethylene glycol) PEG_4 spacer to enhance water solubility and improve probes' pharmacokinetic properties. Specific binding of this nanocarrier and competitive inhibition were assessed in vitro in RAGE-expressing cells using flow cytometry. In addition, the sensitivity, organ specificity and biodistribution were studied in vivo with PET-CT and fluorescence

imaging. Finally, the feasibility of this probe for targeted RAGE imaging was successfully evaluated in the preclinical model of hindlimb ischemia. ^{64}Cu-Rho-G_4-CML was retained in ischemic muscles expressing RAGE as demonstrated using PET-CT, fluorescence and Cerenkov luminescence imaging (Figure 7). This study demonstrated that the integration of both nuclear and fluorescent labels broadened the RAGE imaging probe's utility, allowing its use in cellular analyses, live animal PET imaging, and histological evaluations (Woźniak et al., 2021).

Few years later, the same group used a slightly modified probe (^{64}Cu-Cy5-G_4-CML) for in vivo quantitative multimodal imaging of RAGE expression in prostate cancer (Konopka et al., 2020). The probe's binding affinity and targeting specificity were first assessed in androgen-dependent (LNCaP) and androgen-independent (DU145) prostate cancer cells using flow cytometry and confocal microscopy. Following in vitro studies performed to confirm specific RAGE targeting and establish dissociation constant (KD) between 360 and 540 nM, in vivo experiments were performed in immunocompromised nude mice bearing LNCaP or DU145 subcutaneous xenografts. In vivo PET-CT images of prostate cancer xenografts revealed favorable kinetics, rapid blood clearance, and a nonhomogeneous, enhanced uptake in tumors

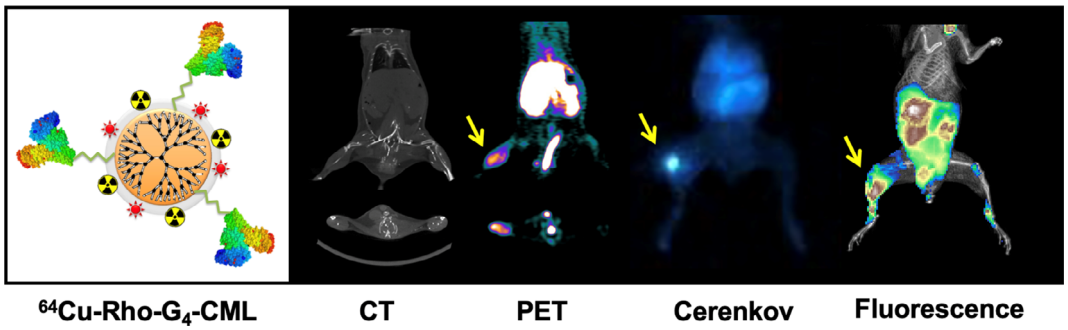

FIGURE 7 Representative positron emission tomography (PET), Cerenkov luminescence and fluorescence images of RAGE expression in a mouse subjected to surgical ligation of right femoral artery to induce hindlimb ischemia followed by an inflammatory response. The animal was injected intravenously with multimodal RAGE-targeted G4-dendrimer nanoparticles (^{64}Cu-Rho-G_4-CML) conjugated with Nϵ-carboxymethyl-lysine (CML) and labeled with rhodamine and radioactive Copper-64.

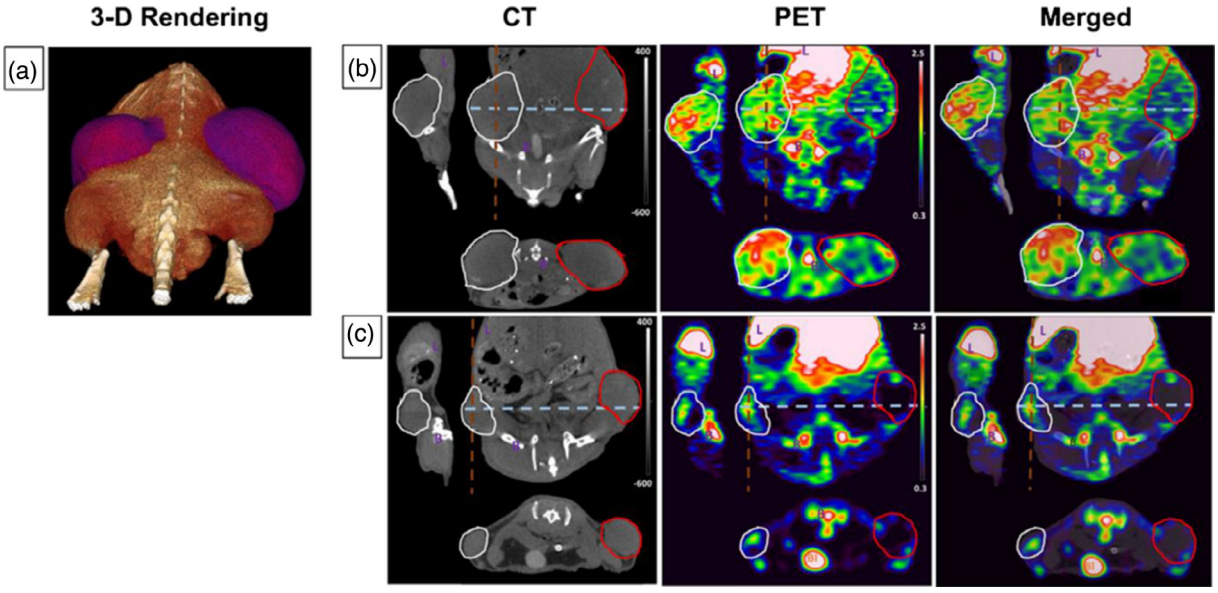

FIGURE 8 Representative PET-CT imaging of RAGE in prostate cancer. Representative ^{64}Cu-Cy5-G_4-CML PET-CT images are demonstrated. A 3D PET-CT rendering of a LNCaP tumor-bearing mouse is presented (a) and subsequent slice views of CT, PET, and merged PET-CT images are shown for LNCaP (b) and DU145 (c). Left-sided (right-sided on screen) tumor is circled in red, right-sided tumors are circled in gray. Cross-sectional views are presented, coronal views are located in the center, sagittal views shown on the top left side (brown dashed line) and axial view showed on the bottom (gray dashed line) of each image. Liver is noted with L and bone noted with B. Reproduced with permission from Konopka et al. (2020).

(Figure 8), which varied based on cell type and tumor size with mean uptake between 0.5 and 1.4 %ID/g. In this study, in addition to a conventional quantification of a mean and maximal radiotracer uptake within the defined tumor volume-of-interest (VOI), due to the heterogeneous uptake patterns observed both within and between different tumor types, additional image analysis was performed which allowed the quantification of tumor heterogeneity. The image heterogeneity analysis was performed to evaluate whether different tumor types can be identified by unique texture features and whether texture features change with the tumor's progression. Both hierarchical clustering and principal component analysis demonstrated that by combination of RAGE-targeted nanoparticle imaging with a novel image analysis, it was possible to identify different tumor types (LNCaP and DU145). Finally, authors demonstrated that it was possible to employ RAGE-targeted multimodal probe for correlation between probe retention, RAGE expression and human prostate cancer grading based on a Gleason scale.

5 | CONCLUSION

Dysregulation of the RAGE expression and function has been implicated in the etiology and progression of several diseases, including diabetes, AD, CVD, and cancer. Studies have demonstrated that RAGE activation can lead to the production of pro-inflammatory cytokines, activation of NF-κB, and promotion of oxidative stress, all of which contribute to the pathogenesis of these diseases. Additionally, RAGE has been shown to interact with various ligands, including AGEs, S100 proteins, and amyloid beta, all of which are associated with disease pathogenesis. Considering the importance of the RAGE/AGE axis and its biology in the diseases' initiation and progression, it became clear that there is a need to develop both RAGE-targeted imaging strategies and therapeutic interventions which can provide novel treatments for these diseases.

Utilizing molecular imaging holds tremendous potential for expediting, streamlining, and reducing the expenses involved in providing and enhancing healthcare, ultimately leading to a significant improvement in the overall quality of life. However, in order to fully achieve these benefits, experts in the field, both from academic and industrial sectors, must focus their research efforts on various areas. These include developing new imaging probes to enhance our comprehension of biology and organ function, designing hybrid imaging instruments for multimodal imaging approaches, implementing theranostic strategies in clinical practice, utilizing molecular imaging for drug discovery and evaluation, and translating research from laboratory to clinical settings, which includes investing in infrastructure and providing clinical scientists with adequate training.

Molecular imaging of RAGE/AGE axis has shown great potential in various fields of medicine, including neurology, cardiology, and oncology. The noninvasive nature of imaging techniques such as PET, single-photon emission computed tomography (SPECT) and optical methods allows for early detection of RAGE-related pathologies, such as AD, atherosclerosis, and cancer, and can aid physicians in the patient triage and outcomes prognostication. Furthermore, the ability to visualize RAGE expression in vivo provides a valuable tool for monitoring disease progression, evaluating treatment efficacy, and developing novel therapeutics. Additionally, recent advances in imaging technology, such as the development of radiolabeled RAGE ligands, have enabled the quantification of RAGE expression, which can aid in patient stratification and personalized medicine.

Incorporating postgenomic techniques such as molecular biology, nanomedicine, proteomics, protein–protein interactions, and reporter genes has significantly advanced the discovery and development of molecular imaging probes, including RAGE-targeted agents. The question addressed here is whether the development of RAGE imaging strategies has been predominantly oriented toward target validation or toward impacting a particular disease.

Target validation is a crucial step in the development process of molecular imaging probes as a well-characterized target is essential for the probe to have diagnostic value. However, even with a validated target, molecular imaging probes must also demonstrate their potential to monitor disease progression and the efficacy of therapeutic intervention noninvasively to have a significant impact on patient care. Without such potential, these probes may not achieve their maximum clinical potential and regulatory approval. To put it differently, as per the recommendations of the FDA, producing visually stunning images alone is not sufficient for regulatory approval; the probe must offer a tangible benefit to the patient's outcome.

In conclusion, despite the fact that imaging of RAGE has a great potential for improving the diagnosis, monitoring, and treatment of various pathologies, further research and development of imaging techniques and molecular probes following careful target validation are necessary to fully realize the clinical applicability of RAGE imaging.

AUTHOR CONTRIBUTIONS

Iwona T. Dobrucki: Conceptualization (supporting); project administration (supporting); resources (equal); writing – original draft (equal); writing – review and editing (equal). **Angelo Miskalis:** Writing – original draft (supporting). **Michael Nelappana:** Formal analysis (equal); investigation (equal); writing – review and editing (equal). **Catherine Applegate:** Investigation (equal); methodology (equal); writing – review and editing (equal). **Marcin Wozniak:** Investigation (equal); methodology (equal). **Andrzej Czerwinski:** Conceptualization (equal); methodology (equal); resources (equal). **Leszek Kalinowski:** Funding acquisition (equal); project administration (equal); resources (equal); writing – review and editing (equal). **Lawrence W. Dobrucki:** Conceptualization (lead); project administration (lead); resources (equal); supervision (equal); visualization (equal); writing – original draft (equal); writing – review and editing (equal).

ACKNOWLEDGMENTS

Some of the work described in this manuscript was carried out in part in the Biomedical Imaging Center at the Beckman Institute for Advanced Science and Technology at the University of Illinois at Urbana-Champaign.

FUNDING INFORMATION

This research was funded in part by the Pilot Grant from Cancer Center at Illinois (Lawrence W. Dobrucki), Polish Ministry of Education and Science, grants no. 10/E-389/SPUB/SP/2020 (Leszek Kalinowski) and DIR/WK/2017/01 (Leszek Kalinowski, Lawrence W. Dobrucki) with the Digitalization Platform of Imaging Data of BBMRI.pl.

CONFLICT OF INTEREST STATEMENT

The authors declare no conflicts of interest.

DATA AVAILABILITY STATEMENT

Data sharing is not applicable to this article as no new data were created or analyzed in this study.

ORCID

Iwona T. Dobrucki https://orcid.org/0000-0002-4428-3060
Angelo Miskalis https://orcid.org/0000-0001-5788-4060
Michael Nelappana https://orcid.org/0000-0003-3470-755X
Catherine Applegate https://orcid.org/0000-0003-1255-0184
Marcin Wozniak https://orcid.org/0000-0002-7129-2202
Leszek Kalinowski https://orcid.org/0000-0001-7270-1592
Lawrence W. Dobrucki https://orcid.org/0000-0002-6807-217X

RELATED WIREs ARTICLES

Multifunctional nanoparticle composites: Progress in the use of soft and hard nanoparticles for drug delivery and imaging

REFERENCES

Allmen, E. U.-v., Koch, M., Fritz, G., & Legler, D. F. (2008). V domain of RAGE interacts with AGEs on prostate carcinoma cells. *The Prostate*, *68*(7), 748–758.

Anzilotti, S., Giampà, C., Laurenti, D., Perrone, L., Bernardi, G., Melone, M. A. B., & Fusco, F. R. (2012). Immunohistochemical localization of receptor for advanced glycation end (RAGE) products in the R6/2 mouse model of Huntington's disease. *Brain Research Bulletin*, *87*(2–3), 350–358.

Arumugam, T., Ramachandran, V., Gomez, S. B., Schmidt, A. M., & Logsdon, C. D. (2012). S100P-derived RAGE antagonistic peptide reduces tumor growth and metastasis. *Clinical Cancer Research: An Official Journal of the American Association for Cancer Research*, *18*(16), 4356–4364.

Basu, S., Kwee, T. C., Surti, S., Akin, E. A., Yoo, D., & Alavi, A. (2011). Fundamentals of PET and PET/CT imaging. *Annals of the New York Academy of Sciences*, *1228*, 1–18.

Bekircan-Kurt, C. E., Üçeyler, N., & Sommer, C. (2014). Cutaneous activation of rage in nonsystemic vasculitic and diabetic neuropathy. *Muscle & Nerve*, *50*(3), 377–383.

Bengel, F. M. (2009). Clinical cardiovascular molecular imaging. *Journal of Nuclear Medicine: Official Publication, Society of Nuclear Medicine*, *50*(6), 837–840.

Bongarzone, S., Savickas, V., Luzi, F., & Gee, A. D. (2017). Targeting the receptor for advanced glycation endproducts (RAGE): A medicinal chemistry perspective. *Journal of Medicinal Chemistry.*, *60*, 7213–7232. https://doi.org/10.1021/acs.jmedchem.7b00058

Boone, B. A., Orlichenko, L., Schapiro, N. E., Loughran, P., Gianfrate, G. C., Ellis, J. T., Singhi, A. D., Kang, R., Tang, D., Lotze, M. T., & Zeh, H. J. (2015). The receptor for advanced glycation end products (RAGE) enhances autophagy and neutrophil extracellular traps in pancreatic cancer. *Cancer Gene Therapy*, *22*(6), 326–334.

Brabletz, T., Raghu Kalluri, M., Nieto, A., & Weinberg, R. A. (2018). EMT in cancer. *Nature Reviews. Cancer*, *18*(2), 128–134.

Brownlee, M. (2001). Biochemistry and molecular cell biology of diabetic complications. *Nature*, *414*(6865), 813–820.

Bu, D.-X., Rai, V., Shen, X., Rosario, R., Yan, L., D'Agati, V., Yan, S. F., Friedman, R. A., Nuglozeh, E., & Schmidt, A. M. (2010). Activation of the ROCK1 branch of the transforming growth factor-β pathway contributes to RAGE-dependent acceleration of atherosclerosis in diabetic ApoE-null mice. *Circulation Research*, *106*(6), 1040–1051.

Bucciarelli, L. G., Ananthakrishnan, R., Hwang, Y. C., Kaneko, M., Song, F., Sell, D. R., Strauch, C., Monnier, V. M., Yan, S. F., Schmidt, A. M., & Ramasamy, R. (2008). RAGE and modulation of ischemic injury in the diabetic myocardium. *Diabetes*, *57*(7), 1941–1951.

Bucciarelli, L. G., Thoralf Wendt, W. Q., Yan, L., Lalla, E., Rong, L. L., Goova, M. T., et al. (2002). RAGE blockade stabilizes established atherosclerosis in diabetic apolipoprotein E–null mice. *Circulation*, *106*(22), 2827–2835.

Burke, A. P., Kolodgie, F. D., Zieske, A., Fowler, D. R., Weber, D. K., Jacob Varghese, P., Farb, A., & Virmani, R. (2004). Morphologic findings of coronary atherosclerotic plaques in diabetics. *Arteriosclerosis, Thrombosis, and Vascular Biology*, *24*(7), 1266–1271.

Burstein, A. H., Brantley, S. J., Dunn, I., Altstiel, L. D., & Schmith, V. (2019). Assessment of Azeliragon QTc liability through integrated, model-based concentration QTc analysis. *Clinical Pharmacology in Drug Development*, *8*(4), 426–435.

Burstein, A. H., Grimes, I., Galasko, D. R., Aisen, P. S., Sabbagh, M., & Mjalli, A. M. M. (2014). Effect of TTP488 in patients with mild to moderate Alzheimer's disease. *BMC Neurology*, *14*(1), 12.

Businaro, R., Leone, S., Fabrizi, C., Sorci, G., Donato, R., Lauro, G. M., & Fumagalli, L. (2006). S100B protects LAN-5 neuroblastoma cells against Aβ amyloid-induced neurotoxicity via RAGE engagement at low doses but increases Aβ amyloid neurotoxicity at high doses. *Journal of Neuroscience Research*, *83*(5), 897–906.

Cai, X.-G., Xia, J.-R., Li, W.-D., Lu, F.-L., Liu, J., Lu, Q., & Zhi, H. (2014). Anti-fibrotic effects of specific-siRNA targeting of the receptor for advanced glycation end products in a rat model of experimental hepatic fibrosis. *Molecular Medicine Reports*, *10*(1), 306–314.

Cary, B. P., Brooks, A. F., Fawaz, M. V., Drake, L. R., Desmond, T. J., Sherman, P., Quesada, C. A., & Scott, P. J. H. (2016). Synthesis and evaluation of [18F]RAGER: A first generation small-molecule PET radioligand targeting the receptor for advanced glycation end-products. *ACS Chemical Neuroscience*, *7*(3), 391–398.

Casula, M., Iyer, A. M., Spliet, W. G. M., Anink, J. J., Steentjes, K., Sta, M., Troost, D., & Aronica, E. (2011). Toll-like receptor signaling in amyotrophic lateral sclerosis spinal cord tissue. *Neuroscience*, *179*(April), 233–243.

Chandra, K. P., Shiwalkar, A., Kotecha, J., Thakkar, P., Srivastava, A., Chauthaiwale, V., Sharma, S. K., Cross, M. R., & Dutt, C. (2009). Phase I clinical studies of the advanced glycation end-product (AGE)-breaker TRC4186. *Clinical Drug Investigation*, *29*(9), 559–575.

Chen, N. X., Srinivasan, S., O'Neill, K., Nickolas, T. L., Wallace, J. M., Allen, M. R., Metzger, C. E., Creecy, A., Avin, K. G., & Moe, S. M. (2020). Effect of advanced glycation end-products (AGE) lowering drug ALT-711 on biochemical, vascular, and bone parameters in a rat model of CKD-MBD. *Journal of Bone and Mineral Research: The Official Journal of the American Society for Bone and Mineral Research*, *35*(3), 608–617.

Chen, X., Zhang, L., Zhang, I. Y., Liang, J., Wang, H., Ouyang, M., Shihua, W., et al. (2014). RAGE expression in tumor-associated macrophages promotes angiogenesis in glioma. *Cancer Research*, *74*(24), 7285–7297.

Cheng, G., Wang, L.-L., Long, L., Liu, H.-Y., Cui, H., Qu, W.-S., & Li, S. (2007). Beneficial effects of C36, a novel breaker of advanced glycation endproducts cross-links, on the cardiovascular system of diabetic rats. *British Journal of Pharmacology*, *152*(8), 1196–1206.

Chuah, Y. K., Basir, R., Talib, H., Tie, T. H., & Nordin, N. (2013). Receptor for advanced glycation end products and its involvement in inflammatory diseases. *International Journal of Inflammation*, *2013*, 1–15.

Cipollone, F., Iezzi, A., Fazia, M., Zucchelli, M., Pini, B., Cuccurullo, C., De Cesare, D., et al. (2003). The receptor RAGE as a progression factor amplifying arachidonate-dependent inflammatory and proteolytic response in human atherosclerotic plaques. *Circulation*, *108*(9), 1070–1077.

Coughlan, M. T., Yap, F. Y. T., Tong, D. C. K., Andrikopoulos, S., Gasser, A., Thallas-Bonke, V., Webster, D. E., Miyazaki, J.-i., Kay, T. W., Slattery, R. M., Kaye, D. M., Drew, B. G., Kingwell, B. A., Fourlanos, S., Groop, P.-H., Harrison, L. C., Knip, M., & Forbes, J. M. (2011). Advanced glycation end products are direct modulators of β-cell function. *Diabetes*, *60*(10), 2523–2532.

Coussens, L. M., & Werb, Z. (2002). Inflammation and cancer. *Nature*, *420*(6917), 860–867.

Criscuolo, C., Fontebasso, V., Middei, S., Stazi, M., Ammassari-Teule, M., Yan, S. S., & Origlia, N. (2017). Entorhinal cortex dysfunction can be rescued by inhibition of microglial RAGE in an Alzheimer's disease mouse model. *Scientific Reports*, *7*(1), 42370.

Dana, H., Chalbatani, G. M., Mahmoodzadeh, H., Karimloo, R., Rezaiean, O., Moradzadeh, A., Mehmandoost, N., et al. (2017). Molecular mechanisms and biological functions of siRNA. *International Journal of Biomedical Science: IJBS*, *13*(2), 48–57.

Datta, P., Kallur, L., & Abraham, E. C. (2008). Reversal of chaperone activity loss of glycated αA-crystallin by a crosslink breaker. *Molecular and Cellular Biochemistry*, *315*(1–2), 137–142.

De Silva, R. A., Jain, S., Lears, K. A., Chong, H. S., Kang, C. S., Sun, X., & Rogers, B. E. (2012). Copper-64 radiolabeling and biological evaluation of bifunctional chelators for radiopharmaceutical development. *Nuclear Medicine and Biology*, *39*(8), 1099–1104.

de Visser, K. E., Eichten, A., & Coussens, L. M. (2006). Paradoxical roles of the immune system during cancer development. *Nature Reviews. Cancer*, *6*(1), 24–37.

Deane, R., Singh, I., Sagare, A. P., Bell, R. D., Ross, N. T., LaRue, B., Love, R., Perry, S., Paquette, N., Deane, R. J., Thiyagarajan, M., Zarcone, T., Fritz, G., Friedman, A. E., Miller, B. L., & Zlokovic, B. V. (2012). A multimodal RAGE-specific inhibitor reduces amyloid β–mediated brain disorder in a mouse model of Alzheimer disease. *The Journal of Clinical Investigation*, *122*(4), 1377–1392.

Delgado-Andrade, C. (2016). Carboxymethyl-lysine: Thirty years of investigation in the field of AGE formation. *Food & Function*, *7*(1), 46–57.

Di Pino, A., Urbano, F., Zagami, R. M., Filippello, A., Di Mauro, S., Piro, S., Purrello, F., & Rabuazzo, A. M. (2016). Low endogenous secretory receptor for advanced glycation end-products levels are associated with inflammation and carotid atherosclerosis in prediabetes. *The Journal of Clinical Endocrinology and Metabolism*, *101*(4), 1701–1709.

Diamanti-Kandarakis, E., Palimeri, S., & Palioura, E. (2015). Current perspectives on the health risks associated with the consumption of advanced glycation end products: Recommendations for dietary management. *Diabetes, Metabolic Syndrome and Obesity: Targets and Therapy*, *8*(September), 415.

Dobrucki, L. W., de Muinck, E. D., Lindner, J. R., & Sinusas, A. J. (2010). Approaches to multimodality imaging of angiogenesis. *Journal of Nuclear Medicine: Official Publication, Society of Nuclear Medicine*, *51*(Suppl 1), 66S–79S.

Dobrucki, L. W., Pan, D., & Smith, A. M. (2015). Multiscale imaging of nanoparticle drug delivery. *Current Drug Targets*, *16*(6), 560–570.

Dobrucki, L. W., & Sinusas, A. J. (2010). PET and SPECT in cardiovascular molecular imaging. *Nature Reviews. Cardiology*, *7*(1), 38–47.

Drake, L. R., Brooks, A. F., Stauff, J., Sherman, P. S., Arteaga, J., Koeppe, R. A., Reed, A., Montavon, T. J., Skaddan, M. B., & Scott, P. J. H. (2020). Strategies for PET imaging of the receptor for advanced glycation endproducts (RAGE). *Journal of Pharmaceutical and Biomedical Analysis*, *10*(5), 452–465.

Drake, L., & Scott, P. (2018). A small molecule radioligand for the intracellular face of RAGE. *Journal of Nuclear Medicine*, *59*(Suppl 1), 1018.

Dukic-Stefanovic, S., Gasic-Milenkovic, J., Deuther-Conrad, W., & Münch, G. (2003). Signal transduction pathways in mouse microglia N-11 cells activated by advanced glycation endproducts (AGEs). *Journal of Neurochemistry*, *87*(1), 44–55.

Egaña-Gorroño, L., López-Díez, R., Yepuri, G., Ramirez, L. S., Reverdatto, S., Gugger, P. F., Shekhtman, A., Ramasamy, R., & Schmidt, A. M. (2020). Receptor for advanced glycation end products (RAGE) and mechanisms and therapeutic opportunities in diabetes and cardiovascular disease: Insights from human subjects and animal models. *Frontiers in Cardiovascular Medicine*, *7*(March), 1–15. https://doi.org/10.3389/fcvm.2020.00037

Fang, F., Lue, L.-F., Yan, S., Hongwei, X., Luddy, J. S., Chen, D., Walker, D. G., et al. (2010). RAGE-dependent signaling in microglia contributes to neuroinflammation, Aβ accumulation, and impaired learning/memory in a mouse model of Alzheimer's disease. *The FASEB Journal*, *24*(4), 1043–1055.

Forbes, J. M., Yee, L. T. L., Thallas, V., Lassila, M., Candido, R., Jandeleit-Dahm, K. A., Thomas, M. C., Burns, W. C., Deemer, E. K., Thorpe, S. R., Cooper, M. E., & Allen, T. J. (2004). Advanced glycation end product interventions reduce diabetes-accelerated atherosclerosis. *Diabetes*, *53*(7), 1813–1823.

Freixes, M., Rodríguez, A., Dalfó, E., & Ferrer, I. (2006). Oxidation, glycoxidation, lipoxidation, nitration, and responses to oxidative stress in the cerebral cortex in Creutzfeldt–Jakob disease. *Neurobiology of Aging*, *27*(12), 1807–1815.

Fritz, G. (2011). RAGE: A single receptor fits multiple ligands. *Trends in Biochemical Sciences*, *36*(12), 625–632.

Fukami, K., Yamagishi, S.-I., & Okuda, S. (2014). Role of AGEs-RAGE system in cardiovascular disease. *Current Pharmaceutical Design*, *20*(14), 2395–2402.

Galasko, D., Bell, J., Mancuso, J. Y., Kupiec, J. W., Sabbagh, M. N., van Dyck, C., Thomas, R. G., & Aisen, P. S. (2014). Clinical trial of an inhibitor of RAGE-A interactions in Alzheimer disease. *Neurology*, *82*(17), 1536–1542.

Garay-Sevilla, M. E., Luevano-Contreras, C., & Chapman-Novakofski, K. (2016). Nutritional modulation of advanced glycation end products. In M. Malavolta & E. Mocchegiani (Eds.), *Molecular basis of nutrition and aging* (pp. 263–276). Elsevier.

Han, Y. T., Choi, G.-I., Son, D., Kim, N.-J., Yun, H., Lee, S., Chang, D. J., Hong, H.-S., Kim, H., Ha, H.-J., Kim, Y.-H., Park, H.-J., Lee, J., & Suh, Y.-G. (2012). Ligand-based design, synthesis, and biological evaluation of 2-aminopyrimidines, a novel series of receptor for advanced glycation end products (RAGE) inhibitors. *Journal of Medicinal Chemistry*, *55*(21), 9120–9135.

Han, Y. T., Kim, K., Choi, G.-I., An, H., Son, D., Kim, H., Ha, H.-J., Son, J.-H., Chung, S.-J., Park, H.-J., Lee, J., & Suh, Y.-G. (2014). Pyrazole-5-carboxamides, novel inhibitors of receptor for advanced glycation end products (RAGE). *European Journal of Medicinal Chemistry*, *79*(May), 128–142.

Han, Y. T., Kim, K., Son, D., An, H., Kim, H., Lee, J., Park, H.-J., Lee, J., & Suh, Y.-G. (2015). Fine tuning of 4,6-bisphenyl-2-(3-alkoxyanilino)pyrimidine focusing on the activity-sensitive aminoalkoxy moiety for a therapeutically useful inhibitor of receptor for advanced glycation end products (RAGE). *Bioorganic & Medicinal Chemistry*, *23*(3), 579–587.

Harcourt, B. E., Sourris, K. C., Coughlan, M. T., Walker, K. Z., Dougherty, S. L., Andrikopoulos, S., Morley, A. L., Thallas-Bonke, V., Chand, V., Penfold, S. A., de Courten, M. P. J., Thomas, M. C., Kingwell, B. A., Bierhaus, A., Cooper, M. E., de Courten, B., & Forbes, J. M. (2011). Targeted reduction of advanced glycation improves renal function in obesity. *Kidney International*, *80*(2), 190–198.

Harja, E., De-Xiu, B., Hudson, B. I., Chang, J. S., Shen, X., Hallam, K., Kalea, A. Z., et al. (2008). Vascular and inflammatory stresses mediate atherosclerosis via RAGE and its ligands in apoE−/− mice. *The Journal of Clinical Investigation*, *118*(1), 183–194.

Hartog, J. W. L., Willemsen, S., van Veldhuisen, D. J., Posma, J. L., van Wijk, L. M., Hummel, Y. M., Hillege, H. L., & Voors, A. A. (2011). Effects of alagebrium, an advanced glycation endproduct breaker, on exercise tolerance and cardiac function in patients with chronic heart failure. *European Journal of Heart Failure*, *13*(8), 899–908.

Healey, G. D., Frostell, A., Fagge, T., Gonzalez, D., & Steven Conlan, R. (2019). A RAGE-targeted antibody-drug conjugate: Surface plasmon resonance as a platform for accelerating effective ADC design and development. *Antibodies*, *8*(1), 7.

Healey, G. D., Pan-Castillo, B., Garcia-Parra, J., Davies, J., Roberts, S., Jones, E., Dhar, K., Nandanan, S., Tofazzal, N., Piggott, L., Clarkson, R., Seaton, G., Frostell, A., Fagge, T., McKee, C., Margarit, L., Conlan, R. S., & Gonzalez, D. (2019). Antibody drug conjugates against the receptor for advanced glycation end products (RAGE), a novel therapeutic target in endometrial cancer. *Journal for Immunotherapy of Cancer*, *7*(1), 280.

Hong, J., Sook Hee, K., Lee, M. S., Jeong, J. H., Mok, H., Choi, D., & Kim, S. H. (2014). Cardiac RNAi therapy using RAGE siRNA/deoxycholic acid-modified polyethylenimine complexes for myocardial infarction. *Biomaterials*, *35*(26), 7562–7573.

Hong, Y., Shen, C., Yin, Q., Sun, M., Ma, Y., & Liu, X. (2016). Effects of RAGE-specific inhibitor FPS-ZM1 on amyloid-β metabolism and AGEs-induced inflammation and oxidative stress in rat hippocampus. *Neurochemical Research*, *41*(5), 1192–1199.

Hori, O., Brett, J., Slattery, T., Cao, R., Zhang, J., Chen, J. X., Nagashima, M., Lundh, E. R., Vijay, S., Nitecki, D., Morser, J., Stern, D., & Schmidt, A. M. (1995). The receptor for advanced glycation end products (RAGE) is a cellular binding site for amphoterin. *The Journal of Biological Chemistry*, *270*(43), 25752–25761.

Huang, C.-Y., Chiang, S.-F., Chen, W. T.-L., Ke, T.-W., Chen, T.-W., You, Y.-S., Chen-Yu Lin, K. S., Chao, C., & Huang, C.-Y. (2018). HMGB1 promotes ERK-mediated mitochondrial Drp1 phosphorylation for chemoresistance through RAGE in colorectal cancer. *Cell Death & Disease*, *9*(10), 1004.

Huttunen, H. J., Kuja-Panula, J., & Rauvala, H. (2002). Receptor for advanced glycation end products (RAGE) signaling induces CREB-dependent chromogranin expression during neuronal differentiation. *The Journal of Biological Chemistry*, *277*(41), 38635–38646.

Huttunen, H. J., Kuja-Panula, J., Sorci, G., Agneletti, A. L., Donato, R., & Rauvala, H. (2000). Coregulation of neurite outgrowth and cell survival by amphoterin and S100 proteins through receptor for advanced glycation end products (RAGE) activation. *The Journal of Biological Chemistry*, *275*(51), 40096–40105.

Ishibashi, Y., Matsui, T., Takeuchi, M., & Yamagishi, S. (2012). Metformin inhibits advanced glycation end products (AGEs)-induced growth and VEGF expression in MCF-7 breast cancer cells by suppressing AGEs receptor expression via AMP-activated protein kinase. *Hormone and Metabolic Research = Hormon- Und Stoffwechselforschung = Hormones et Metabolisme*, *45*(5), 387–390.

Johnson, L. L., Tekabe, Y., Kollaros, M., Eng, G., Bhatia, K., Li, C., Krueger, C. G., Shanmuganayagam, D., & Schmidt, A. M. (2014). Imaging RAGE expression in atherosclerotic plaques in hyperlipidemic pigs. *EJNMMI Research*, *4*(1), 26.

Joshi, D., Gupta, R., Dubey, A., Shiwalkar, A., Pathak, P., Gupta, R. C., Chauthaiwale, V., & Dutt, C. (2009). TRC4186, a novel AGE-breaker, improves diabetic cardiomyopathy and nephropathy in Ob-ZSF1 model of type 2 diabetes. *Journal of Cardiovascular Pharmacology*, *54*(1), 72–81.

Jud, P., & Sourij, H. (2019). Therapeutic options to reduce advanced glycation end products in patients with diabetes mellitus: A review. *Diabetes Research and Clinical Practice*, *148*(February), 54–63.

Judenhofer, M. S., & Cherry, S. R. (2013). Applications for preclinical PET/MRI. *Seminars in Nuclear Medicine*, *43*(1), 19–29.

Juranek, J., Ray, R., Banach, M., & Rai, V. (2015). Receptor for advanced glycation end-products in neurodegenerative diseases. *Reviews in the Neurosciences*, *26*(6), 691–698.

Kanasty, R., Dorkin, J. R., Vegas, A., & Anderson, D. (2013). Delivery materials for siRNA therapeutics. *Nature Materials*, *12*(11), 967–977.

Kang, R., Tang, D., Schapiro, N. E., Livesey, K. M., Farkas, A., Loughran, P., Bierhaus, A., Lotze, M. T., & Zeh, H. J. (2010). The receptor for advanced glycation end products (RAGE) sustains autophagy and limits apoptosis, promoting pancreatic tumor cell survival. *Cell Death and Differentiation*, *17*(4), 666–676.

Kessenbrock, K., Plaks, V., & Werb, Z. (2010). Matrix metalloproteinases: Regulators of the tumor microenvironment. *Cell*, *141*(1), 52–67.

Kim, H. S., Chung, W., Kim, A. J., Ro, H., Chang, J. H., Lee, H. H., & Jung, J. Y. (2013). Circulating levels of soluble receptor for advanced glycation end product are inversely associated with vascular calcification in patients on haemodialysis independent of S100A12 (EN-RAGE) levels. *Nephrology*, *18*(12), 777–782.

Kim, J., & Bae, J.-S. (2016). Tumor-associated macrophages and neutrophils in tumor microenvironment. *Mediators of Inflammation*, *2016*, 1–11.

Kislinger, T., Caifeng, F., Birgit Huber, W. Q., Taguchi, A., Du Yan, S., Hofmann, M., et al. (1999). N ε-(carboxymethyl)lysine adducts of proteins are ligands for receptor for advanced glycation end products that activate cell signaling pathways and modulate gene expression. *The Journal of Biological Chemistry*, *274*(44), 31740–31749.

Konopka, C. J., Wozniak, M., Hedhli, J., Ploska, A., Schwartz-Duval, A., Siekierzycka, A., Pan, D., et al. (2018). Multimodal imaging of the receptor for advanced glycation end-products with molecularly targeted nanoparticles. *Theranostics*, *8*(18), 5012–5024.

Konopka, C. J., Woźniak, M., Hedhli, J., Siekierzycka, A., Skokowski, J., Pęksa, R., Matuszewski, M., Munirathinam, G., Kajdacsy-Balla, A., Dobrucki, I. T., Kalinowski, L., & Dobrucki, L. W. (2020). Quantitative imaging of the receptor for advanced glycation end-products in prostate cancer. *European Journal of Nuclear Medicine and Molecular Imaging*, *47*, 2562–2576.

Koulis, C., Kanellakis, P., Pickering, R. J., Tsorotes, D., Murphy, A. J., Gray, S. P., Thomas, M. C., Jandeleit-Dahm, K. A. M., Cooper, M. E., & Allen, T. J. (2014). Role of bone-marrow- and non-bone-marrow-derived receptor for advanced glycation end-products (RAGE) in a mouse model of diabetes-associated atherosclerosis. *Clinical Science*, *127*(7), 485–497.

Koyama, H., Yamamoto, H., & Nishizawa, Y. (2007). RAGE and soluble RAGE: potential therapeutic targets for cardiovascular diseases. *Molecular Medicine*, *13*(11–12), 625–635.

Kwak, T., Drews-Elger, K., Ergonul, A., Miller, P. C., Braley, A., Hwang, G. H., Zhao, D., et al. (2016). Targeting of RAGE-ligand signaling impairs breast cancer cell invasion and metastasis. *Oncogene*, *36*(11), 1559–1572.

Labieniec-Watala, M., & Watala, C. (2015). PAMAM dendrimers: Destined for success or doomed to fail? Plain and modified PAMAM dendrimers in the context of biomedical applications. *Journal of Pharmaceutical Sciences*, *104*(1), 2–14.

Lee, J. H., Park, G., Hong, G. H., Choi, J., & Choi, H. S. (2012). Design considerations for targeted optical contrast agents. *Quantitative Imaging in Medicine and Surgery*, *2*(4), 266–273.

Lee, J.-J., Wang, P.-W., Yang, I.-H., Wu, C.-L., & Chuang, J.-H. (2015). Amyloid-beta mediates the receptor of advanced glycation end product-induced pro-inflammatory response via toll-like receptor 4 signaling pathway in retinal ganglion cell line RGC-5. *The International Journal of Biochemistry & Cell Biology*, *64*(July), 1–10.

Lee, S., Piao, C., Kim, G., Kim, J. Y., Choi, E., & Lee, M. (2018). Production and application of HMGB1 derived recombinant RAGE-antagonist peptide for anti-inflammatory therapy in acute lung injury. *European Journal of Pharmaceutical Sciences: Official Journal of the European Federation for Pharmaceutical Sciences*, *114*(March), 275–284.

Lee, Y. S., Kim, H., Kim, Y.-H., Roh, E. J., Han, H., & Shin, K. J. (2012). Synthesis and structure–activity relationships of tri-substituted thiazoles as RAGE antagonists for the treatment of Alzheimer's disease. *Bioorganic & Medicinal Chemistry Letters*, *22*(24), 7555–7561.

Lei, C., Bo, W., Cao, T., Zhang, S., & Liu, M. (2015). Activation of the high-mobility group box 1 protein-receptor for advanced glycation end-products signaling pathway in rats during neurogenesis after intracerebral hemorrhage. *Stroke: A Journal of Cerebral Circulation*, *46*(2), 500–506.

Li, J., Kokkola, R., Tabibzadeh, S., Yang, R., Ochani, M., Qiang, X., Harris, H. E., Czura, C. J., Wang, H., Ulloa, L., Wang, H., Warren, H. S., Moldawer, L. L., Fink, M. P., Andersson, U., Tracey, K. J., & Yang, H. (2003). Structural basis for the proinflammatory cytokine activity of high mobility group box 1. *Molecular Medicine*, *9*(1–2), 37–45.

Liang, H., Zhong, Y., Zhou, S., & Peng, L. (2011). Knockdown of RAGE expression inhibits colorectal cancer cell invasion and suppresses angiogenesis in vitro and in vivo. *Cancer Letters*, *313*(1), 91–98.

Little, W. C., Zile, M. R., Kitzman, D. W., Gregory Hundley, W., O'Brien, T. X., & DeGroof, R. C. (2005). The effect of alagebrium chloride (ALT-711), a novel glucose cross-link breaker, in the treatment of elderly patients with diastolic heart failure. *Journal of Cardiac Failure*, *11*(3), 191–195.

Liu, R., Cai-Xia, W., Zhou, D., Yang, F., Tian, S., Zhang, L., Zhang, T.-T., & Guan-Hua, D. (2012). Pinocembrin protects against β-amyloid-induced toxicity in neurons through inhibiting receptor for advanced glycation end products (RAGE)-independent signaling pathways and regulating mitochondrion-mediated apoptosis. *BMC Medicine*, *10*(1), 105.

Liu, Y., Manli, Y., Zhang, Z., Yunhua, Y., Chen, Q., Zhang, W., & Zhao, X. (2016). Blockade of receptor for advanced glycation end products protects against systolic overload-induced heart failure after transverse aortic constriction in mice. *European Journal of Pharmacology*, *791*(November), 535–543.

Lue, L.-F., Walker, D. G., Brachova, L., Beach, T. G., Rogers, J., Schmidt, A. M., Stern, D. M., & Du Yan, S. (2001). Involvement of microglial receptor for advanced glycation Endproducts (RAGE) in Alzheimer's disease: Identification of a cellular activation mechanism. *Experimental Neurology*, *171*(1), 29–45.

Luth, H.-J. (2004). Age- and stage-dependent accumulation of advanced glycation end products in intracellular deposits in normal and Alzheimer's disease brains. *Cerebral Cortex*, *15*(2), 211–220.

Malik, P., Chaudhry, N., Mittal, R., & Mukherjee, T. K. (2015). Role of receptor for advanced glycation end products in the complication and progression of various types of cancers. *Biochimica et Biophysica Acta (BBA)—General Subjects*, *1850*(9), 1898–1904.

Mariani, G., Bruselli, L., Kuwert, T., Kim, E. E., Flotats, A., Israel, O., Dondi, M., & Watanabe, N. (2010). A review on the clinical uses of SPECT/CT. *European Journal of Nuclear Medicine and Molecular Imaging*, *37*(10), 1959–1985.

Meghnani, V., Vetter, S. W., & Leclerc, E. (2014). RAGE overexpression confers a metastatic phenotype to the WM115 human primary melanoma cell line. *Biochimica et Biophysica Acta (BBA)—Molecular Basis of Disease*, *1842*(7), 1017–1027.

Mehner, C., Hockla, A., Miller, E., Ran, S., Radisky, D. C., & Radisky, E. S. (2014). Tumor cell-produced matrix metalloproteinase 9 (MMP-9) drives malignant progression and metastasis of basal-like triple negative breast cancer. *Oncotarget*, *5*(9), 2736–2749.

Meng, Q., Xia, C., Fang, J., Rojanasakul, Y., & Jiang, B.-H. (2006). Role of PI3K and AKT specific isoforms in ovarian cancer cell migration, invasion and proliferation through the p70S6K1 pathway. *Cellular Signalling*, *18*(12), 2262–2271.

Metz, V. V., Kojro, E., Rat, D., & Postina, R. (2012). Induction of RAGE shedding by activation of G protein-coupled receptors. *PLoS One*, *7*(7), e41823.

Nahrendorf, M., Sosnovik, D. E., French, B. A., Swirski, F. K., Bengel, F., Sadeghi, M. M., Lindner, J. R., Wu, J. C., Kraitchman, D. L., Fayad, Z. A., & Sinusas, A. J. (2009). Multimodality cardiovascular molecular imaging, part II. *Circulation. Cardiovascular Imaging*, *2*(1), 56–70.

Nasser, M. W., Wani, N. A., Ahirwar, D. K., Powell, C. A., Ravi, J., Elbaz, M., Zhao, H., Padilla, L., Zhang, X., Shilo, K., Ostrowski, M., Shapiro, C., Carson, W. E., III, & Ganju, R. K. (2015). RAGE mediates S100A7-induced breast cancer growth and metastasis by modulating the tumor microenvironment. *Cancer Research*, *75*, 974–985. https://doi.org/10.1158/0008-5472.CAN-14-2161

Neeper, M., Schmidt, A. M., Brett, J., Yan, S. D., Wang, F., Pan, Y. C., Elliston, K., Stern, D., & Shaw, A. (1992). Cloning and expression of a cell surface receptor for advanced glycosylation end products of proteins. *The Journal of Biological Chemistry*, *267*(21), 14998-5004.

Oldfield, M. D., Bach, L. A., Forbes, J. M., Nikolic-Paterson, D., McRobert, A., Thallas, V., Atkins, R. C., Osicka, T., Jerums, G., & Cooper, M. E. (2001). Advanced glycation end products cause epithelial-myofibroblast transdifferentiation via the receptor for advanced glycation end products (RAGE). *The Journal of Clinical Investigation*, *108*(12), 1853–1863.

Ott, C., Jacobs, K., Haucke, E., Santos, A. N., Grune, T., & Simm, A. (2014). Role of advanced glycation end products in cellular signaling. *Redox Biology*, *2*, 411–429.

Palanissami, G., & Paul, S. F. D. (2018). RAGE and its ligands: Molecular interplay between glycation, inflammation, and hallmarks of cancer—A review. *Hormones and Cancer*, *9*(5), 295–325.

Pandey, A. P., & Sawant, K. K. (2016). Polyethylenimine: A versatile, multifunctional non-viral vector for nucleic acid delivery. *Materials Science and Engineering: C*, *68*(November), 904–918.

Park, H., Sook Hee, K., Park, H., Hong, J., Kim, D., Choi, B.-R., Pak, H.-N., et al. (2015). RAGE siRNA-mediated gene silencing provides cardioprotection against ventricular arrhythmias in acute ischemia and reperfusion. *Journal of Controlled Release: Official Journal of the Controlled Release Society*, *217*(November), 315–326.

Park, M.-J., Lee, S. H., Moon, S.-J., Lee, J.-A., Lee, E.-J., Kim, E.-K., Park, J.-S., Lee, J., Min, J.-K., Kim, S. J., Park, S.-H., & Cho, M.-L. (2016). Overexpression of soluble RAGE in mesenchymal stem cells enhances their immunoregulatory potential for cellular therapy in autoimmune arthritis. *Scientific Reports*, *6*(November), 35933.

Paudel, Y. N., Angelopoulou, E., Piperi, C., Othman, I., Aamir, K., & Shaikh, M. F. (2020). Impact of HMGB1, RAGE, and TLR4 in Alzheimer's disease (AD): From risk factors to therapeutic targeting. *Cell*, *9*(2), 383.

Piao, C., Kim, G., Ha, J., & Lee, M. (2019). Inhalable gene delivery system using a cationic RAGE-antagonist peptide for gene delivery to inflammatory lung cells. *ACS Biomaterials Science & Engineering*, *5*(5), 2247–2257.

Ray, R., Juranek, J. K., & Rai, V. (2016). RAGE axis in neuroinflammation, neurodegeneration and its emerging role in the pathogenesis of amyotrophic lateral sclerosis. *Neuroscience and Biobehavioral Reviews*, *62*(March), 48–55.

Reynolds, A., Leake, D., Boese, Q., Scaringe, S., Marshall, W. S., & Khvorova, A. (2004). Rational siRNA design for RNA interference. *Nature Biotechnology*, *22*(3), 326–330.

Sakaguchi, M., Murata, H., Yamamoto, K.-I., Ono, T., Sakaguchi, Y., Motoyama, A., Hibino, T., Kataoka, K., & Huh, N.-H. (2011). TIRAP, an adaptor protein for TLR2/4, transduces a signal from RAGE phosphorylated upon ligand binding. *PLoS One*, *6*(8), e23132.

Schmidt, A. M., Vianna, M., Gerlach, M., Brett, J., Ryan, J., Kao, J., Esposito, C., Hegarty, H., Hurley, W., & Clauss, M. (1992). Isolation and characterization of two binding proteins for advanced glycosylation end products from bovine lung which are present on the endothelial cell surface. *The Journal of Biological Chemistry*, *267*(21), 14987–14997.

Schmidt, A. M., Du Yan, S., Yan, S. F., & Stern, D. M. (2000). The biology of the receptor for advanced glycation end products and its ligands. *Biochimica et Biophysica Acta (BBA)—Molecular Cell Research*, *1498*(2–3), 99–111.

Shang, L., Ananthakrishnan, R., Li, Q., Quadri, N., Abdillahi, M., Zhengbin Zhu, W. Q., et al. (2010). RAGE modulates hypoxia/reoxygenation injury in adult murine cardiomyocytes via JNK and GSK-3β signaling pathways. *PLoS One*, *5*(4), e10092.

Sharaf, H., Matou-Nasri, S., Wang, Q., Rabhan, Z., Al-Eidi, H., Al Abdulrahman, A., & Ahmed, N. (2015). Advanced glycation endproducts increase proliferation, migration and invasion of the breast cancer cell line MDA-MB-231. *Biochimica et Biophysica Acta (BBA)—Molecular Basis of Disease*, *1852*(3), 429–441.

Shekhtman, A., Ramasamy, R., & Schmidt, A. M. (2017). Glycation & the RAGE axis: Targeting signal transduction through DIAPH1. *Expert Review of Proteomics*, *14*(2), 147–156.

Shibata, N., Hirano, A., Hedley-Whyte, T. E., Dal Canto, M. C., Nagai, R., Uchida, K., Horiuchi, S., Kawaguchi, M., Yamamoto, T., & Kobayashi, M. (2002). Selective formation of certain advanced glycation end products in spinal cord astrocytes of humans and mice with superoxide dismutase-1 mutation. *Acta Neuropathologica*, *104*(2), 171–178.

Sievers, E. L., & Senter, P. D. (2013). Antibody-drug conjugates in cancer therapy. *Annual Review of Medicine*, *64*(1), 15–29.

Sims, G. P., Rowe, D. C., Rietdijk, S. T., Herbst, R., & Coyle, A. J. (2010). HMGB1 and RAGE in inflammation and cancer. *Annual Review of Immunology*, *28*(1), 367–388.

Singh, V. P., Bali, A., Singh, N., & Jaggi, A. S. (2014). Advanced glycation end products and diabetic complications. *The Korean Journal of Physiology & Pharmacology*, *18*(1), 1–14.

Sinusas, A. J., Bengel, F., Nahrendorf, M., Epstein, F. H., Wu, J. C., Villanueva, F. S., Fayad, Z. A., & Gropler, R. J. (2008). Multimodality Cardiovascular Molecular Imaging, Part I. *Circulation. Cardiovascular Imaging*, *1*(3), 244–256.

Soro-Paavonen, A., Zhang, W.-Z., Venardos, K., Coughlan, M. T., Harris, E., Tong, D. C. K., Brasacchio, D., Paavonen, K., Chin-Dusting, J., Cooper, M. E., Kaye, D., Thomas, M. C., & Forbes, J. M. (2010). Advanced glycation end-products induce vascular dysfunction via resistance to nitric oxide and suppression of endothelial nitric oxide synthase. *Journal of Hypertension*, *28*(4), 780–788.

Sousa, M. M., Du Yan, S., Stern, D., & Saraiva, M. J. (2000). Interaction of the receptor for advanced glycation end products (RAGE) with transthyretin triggers nuclear transcription factor kB (NF-kB) activation. *Laboratory Investigation*, *80*(7), 1101–1110.

Sparvero, L. J., Asafu-Adjei, D., Kang, R., Tang, D., Amin, N., Im, J., Rutledge, R., Lin, B., Amoscato, A. A., Zeh, H. J., & Lotze, M. T. (2009). RAGE (receptor for advanced glycation endproducts), RAGE ligands, and their role in cancer and inflammation. *Journal of Translational Medicine*, *7*(March), 17.

Sterenczak, K. A., Nolte, I., & Escobar, H. M. (2013). RAGE splicing variants in mammals. *Methods in Molecular Biology*, *963*, 265–276.

Sugaya, K., Fukagawa, T., Matsumoto, K.-I., Mita, K., Takahashi, E.-I., Ando, A., Inoko, H., & Ikemura, T. (1994). Three genes in the human MHC class III region near the junction with the class II: Gene for receptor of advanced glycosylation end products, PBX2 homeobox gene and a notch homolog, human counterpart of mouse mammary tumor gene int-3. *Genomics*, *23*(2), 408–419.

Taguchi, A., Blood, D. C., del Toro, G., Canet, A., Lee, D. C., Qu, W., Tanji, N., Lu, Y., Lalla, E., Fu, C., Hofmann, M. A., Kislinger, T., Ingram, M., Lu, A., Tanaka, H., Hori, O., Ogawa, S., Stern, D. M., & Schmidt, A. M. (2000). Blockade of RAGE-Amphoterin Signalling suppresses tumour growth and metastases. *Nature*, *405*(6784), 354–360.

Takeuchi, A., Yamamoto, Y., Munesue, S., Harashima, A., Watanabe, T., Yonekura, H., Yamamoto, H., & Tsuchiya, H. (2013). Low molecular weight heparin suppresses receptor for advanced glycation end products-mediated expression of malignant phenotype in human fibrosarcoma cells. *Cancer Science*, *104*(6), 740–749.

Teismann, P., Sathe, K., Bierhaus, A., Leng, L., Martin, H. L., Bucala, R., Weigle, B., Nawroth, P. P., & Schulz, J. B. (2012). Receptor for advanced glycation endproducts (RAGE) deficiency protects against MPTP toxicity. *Neurobiology of Aging*, *33*(10), 2478–2490.

Tekabe, Y., Li, Q., Luma, J., Weisenberger, D., Sedlar, M., Harja, E., Narula, J., & Johnson, L. L. (2010). Noninvasive monitoring the biology of atherosclerotic plaque development with radiolabeled annexin V and matrix metalloproteinase inhibitor in spontaneous atherosclerotic mice. *Journal of Nuclear Cardiology*, *17*, 1073–1081. https://doi.org/10.1007/s12350-010-9276-5

Tekabe, Y., Li, Q., Rosario, R., Sedlar, M., Majewski, S., Hudson, B. I., Einstein, A. J., Schmidt, A. M., & Johnson, L. L. (2008). Development of receptor for advanced glycation end products-directed imaging of atherosclerotic plaque in a murine model of spontaneous atherosclerosis. *Circulation. Cardiovascular Imaging*, *1*(3), 212–219.

Tekabe, Y., Luma, J., Li, Q., Schmidt, A. M., Ramasamy, R., & Johnson, L. L. (2012). Imaging of receptors for advanced glycation end products in experimental myocardial ischemia and reperfusion injury. *JACC Cardiovascular Imaging*, *5*(1), 59–67.

Tekabe, Y., Kollaros, M., Li, C., Zhang, G., Schmidt, A. M., & Johnson, L. (2013). Imaging receptor for advanced glycation end product expression in mouse model of hind limb ischemia. *EJNMMI Research*, *3*(1), 37.

Tekabe, Y., Luma, J., Einstein, A. J., Sedlar, M., Li, Q., Schmidt, A. M., & Johnson, L. L. (2010). A novel monoclonal antibody for RAGE-directed imaging identifies accelerated atherosclerosis in diabetes. *Journal of Nuclear Medicine*, *51*(1), 92–97.

Toprak, C., & Yigitaslan, S. (2019). Alagebrium and complications of diabetes mellitus. *The Eurasian Journal of Medicine*, *51*(3), 285–292.

Tsoporis, J. N., Izhar, S., Leong-Poi, H., Desjardins, J.-F., Huttunen, H. J., & Parker, T. G. (2010). S100B interaction with the receptor for advanced glycation end products (RAGE). *Circulation Research*, *106*(1), 93–101.

Uribarri, J., Woodruff, S., Goodman, S., Cai, W., Chen, X., Pyzik, R., Yong, A., Striker, G. E., & Vlassara, H. (2010). Advanced glycation end products in foods and a practical guide to their reduction in the diet. *Journal of the American Dietetic Association*, *110*(6), 911–916.e12.

van't Veer, L. J., Dai, H., van de Vijver, M. J., He, Y. D., Hart, A. A. M., Mao, M., Peterse, H. L., et al. (2002). Gene expression profiling predicts clinical outcome of breast cancer. *Nature*, *415*(6871), 530–536.

Vaquero, J. J., & Kinahan, P. (2015). Positron emission tomography: Current challenges and opportunities for technological advances in clinical and preclinical imaging systems. *Annual Review of Biomedical Engineering*, *17*, 385–414.

Vasan, S., Zhang, X., Zhang, X., Kapurniotu, A., Bernhagen, J., Teichberg, S., Basgen, J., Wagle, D., Shih, D., Terlecky, I., Bucala, R., Cerami, A., Egan, J., & Ulrich, P. (1996). An agent cleaving glucose-derived protein crosslinks in vitro and in vivo. *Nature*, *382*(6588), 275–278.

Venegas-Pino, D. E., Lagrotteria, A., Wang, P.-W., Morphet, J., Clapdorp, C., Shi, Y., & Werstuck, G. H. (2018). Evidence of extensive atherosclerosis, coronary artery disease and myocardial infarction in the ApoE−/−:Ins2+/Akita mouse fed a Western diet. *Atherosclerosis*, *275*-(August), 88–96.

Villarreal, A., Aviles Reyes, R. X., Angelo, M. F., Reines, A. G., & Ramos, A. J. (2011). S100B alters neuronal survival and dendrite extension via RAGE-mediated NF-κB signaling. *Journal of Neurochemistry*, *117*(2), 321–332.

Wadas, T. J., Wong, E. H., Weisman, G. R., & Anderson, C. J. (2007). Copper chelation chemistry and its role in copper radiopharmaceuticals. *Current Pharmaceutical Design*, *13*(1), 3–16.

Walter, A., Paul-Gilloteaux, P., Plochberger, B., Sefc, L., Verkade, P., Mannheim, J. G., Slezak, P., Unterhuber, A., Marchetti-Deschmann, M., Ogris, M., Bühler, K., Fixler, D., Geyer, S. H., Weninger, W. J., Glösmann, M., Handschuh, S., & Wanek, T. (2020). Correlated multimodal imaging in life sciences: Expanding the biomedical horizon. *Frontiers in Physics*, *8*, 1–28. https://doi.org/10.3389/fphy.2020.00047

Wang, H., Mei, X., Cao, Y., Liu, C., Zhao, Z., Guo, Z., Bi, Y., Shen, Z., Yuan, Y., Guo, Y., Song, C., Bai, L., Wang, Y., & Yu, D. (2017). HMGB1/advanced glycation end products (RAGE) does not aggravate inflammation but promote endogenous neural stem cells differentiation in spinal cord injury. *Scientific Reports*, *7*(1), 10332.

Wang, L., Li, S., & Jungalwala, F. B. (2008). Receptor for advanced glycation end products (RAGE) mediates neuronal differentiation and neurite outgrowth. *Journal of Neuroscience Research*, *86*(6), 1254–1266.

Wang, Z., Li, D.-D., Liang, Y.-Y., Wang, D.-S., & Cai, N.-S. (2002). Activation of astrocytes by advanced glycation end products: Cytokines induction and nitric oxide release. *Acta Pharmacologica Sinica*, *23*(11), 974–980.

Watson, A. M. D., Soro-Paavonen, A., Sheehy, K., Li, J., Calkin, A. C., Koitka, A., Rajan, S. N., Brasacchio, D., Allen, T. J., Cooper, M. E., Thomas, M. C., & Jandeleit-Dahm, K. J. A. (2011). Delayed intervention with AGE inhibitors attenuates the progression of diabetes-accelerated atherosclerosis in diabetic apolipoprotein E knockout mice. *Diabetologia*, *54*(3), 681–689.

Wolffenbuttel, B. H. R., Boulanger, C. M., Crijns, F. R. L., Huijberts, M. S. P., Poitevin, P., Swennen, G. N. M., Vasan, S., Egan, J. J., Ulrich, P., Cerami, A., & Lévy, B. I. (1998). Breakers of advanced glycation end products restore large artery properties in experimental diabetes. *Proceedings of the National Academy of Sciences*, *95*(8), 4630–4634.

Woźniak, M., Konopka, C. J., Płoska, A., Hedhli, J., Siekierzycka, A., Banach, M., Bartoszewski, R., Dobrucki, L. W., Kalinowski, L., & Dobrucki, I. T. (2021). Molecularly targeted nanoparticles: An emerging tool for evaluation of expression of the receptor for advanced glycation end products in a murine model of peripheral artery disease. *Cellular & Molecular Biology Letters*, *26*(1), 10.

Xia, J.-R., Liu, N.-F., & Zhu, N.-X. (2008). Specific siRNA targeting the receptor for advanced glycation end products inhibits experimental hepatic fibrosis in rats. *International Journal of Molecular Sciences*, *9*(4), 638–661.

Xie, J., Reverdatto, S., Frolov, A., Hoffmann, R., Burz, D. S., & Shekhtman, A. (2008). Structural basis for pattern recognition by the receptor for advanced glycation end products (RAGE). *The Journal of Biological Chemistry*, *283*(40), 27255–27269.

Xue, J., Rai, V., Singer, D., Chabierski, S., Xie, J., Reverdatto, S., Burz, D. S., Schmidt, A. M., Hoffmann, R., & Shekhtman, A. (2011). Advanced glycation end product recognition by the receptor for AGEs. *Structure*, *19*(5), 722–732.

Yamagishi, S.-I. (2012). Potential clinical utility of advanced glycation end product cross-link breakers in age- and diabetes-associated disorders. *Rejuvenation Research*, *15*(6), 564–572.

Yang, H., Antoine, D. J., Andersson, U., & Tracey, K. J. (2013). The many faces of HMGB1: Molecular structure-functional activity in inflammation, apoptosis, and chemotaxis. *Journal of Leukocyte Biology*, *93*(6), 865–873.

Yang, M. J., Sook Hee, K., Kim, D., Kim, W. J., Mok, H., Kim, S. H., & Kwon, I. C. (2015). Enhanced cytoplasmic delivery of RAGE siRNA using bioreducible polyethylenimine-based nanocarriers for myocardial gene therapy. *Macromolecular Bioscience*, *15*(12), 1755–1763.

Yang, P.-S., Kim, T.-H., Uhm, J.-S., Park, S., Joung, B., Lee, M.-H., & Pak, H.-N. (2016). High plasma level of soluble RAGE is independently associated with a low recurrence of atrial fibrillation after catheter ablation in diabetic patient. *Europace: European Pacing, Arrhythmias, and Cardiac Electrophysiology*, *18*(11), 1711–1718.

Yao, L., Zhao, H., Tang, H., Liang, J., Liu, L., Dong, H., Zou, F., & Cai, S. (2016). The receptor for advanced glycation end products is required for β-catenin stabilization in a chemical-induced asthma model. *British Journal of Pharmacology*, *173*(17), 2600–2613.

Yatime, L., & Andersen, G. R. (2013). Structural insights into the oligomerization mode of the human receptor for advanced glycation end-products. *The FEBS Journal*, *280*(24), 6556–6568.

Yi, X., Wang, Z., Xiang, H., & Aixi, Y. (2022). Affinity probes based on small-molecule inhibitors for tumor imaging. *Frontiers in Oncology*, *12*, 1–13. https://doi.org/10.3389/fonc.2022.1028493

Yin, C., Li, H., Zhang, B., Liu, Y., Guohua, L., Shijun, L., Sun, L., Qi, Y., Li, X., & Chen, W. (2013). Rage-binding S100A8/A9 promotes the migration and invasion of human breast cancer cells through actin polymerization and epithelial–mesenchymal transition. *Breast Cancer Research and Treatment*, *142*(2), 297–309.

Zeng, D., Lee, N. S., Liu, Y., Zhou, D., Dence, C. S., Wooley, K. L., Katzenellenbogen, J. A., & Welch, M. J. (2012). 64Cu core-labeled nanoparticles with high specific activity via metal-free click chemistry. *ACS Nano*, *6*(6), 5209–5219.

Zha, C., Meng, X., Li, L., Mi, S., Qian, D., Li, Z., Pengfei, W., et al. (2020). Neutrophil extracellular traps mediate the crosstalk between glioma progression and the tumor microenvironment via the HMGB1/RAGE/IL-8 axis. *Cancer Biology and Medicine*, *17*(1), 154–168.

Zhang, J., Shao, S., Han, D., Yuerong, X., Jiao, D., Jieheng, W., Yang, F., et al. (2018). High mobility group box 1 promotes the epithelial-to-mesenchymal transition in prostate cancer PC3 cells via the RAGE/NF-κB signaling pathway. *International Journal of Oncology*, *53*, 659–671. https://doi.org/10.3892/ijo.2018.4420

Zhang, L., Yangyang, X., Sun, J., Chen, W., Zhao, L., Ma, C., Wang, Q., et al. (2017). M2-like tumor-associated macrophages drive vasculogenic mimicry through amplification of IL-6 expression in glioma cells. *Oncotarget*, *8*(1), 819–832.

Zhang, L., Bukulin, M., Kojro, E., Roth, A., Metz, V. V., Fahrenholz, F., Nawroth, P. P., Bierhaus, A., & Postina, R. (2008). Receptor for advanced glycation end products is subjected to protein ectodomain shedding by metalloproteinases. *The Journal of Biological Chemistry*, *283*(51), 35507–35516.

Zhang, Q.-Y., Lin-Qing Wu, T. A. O., Zhang, Y.-F. H., & Lin, X. U. (2015). Autophagy-mediated HMGB1 release promotes gastric cancer cell survival via RAGE activation of extracellular signal-regulated kinases 1/2. *Oncology Reports*, *33*(4), 1630–1638.

Zhang, W., & Liu, H. T. (2002). MAPK signal pathways in the regulation of cell proliferation in mammalian cells. *Cell Research*, *12*(1), 9–18.

Zhu, Q., & Smith, E. A. (2019). Diaphanous-1 affects the nanoscale clustering and lateral diffusion of receptor for advanced glycation end-products (RAGE). *Biochimica et Biophysica Acta (BBA)—Biomembranes*, *1861*(1), 43–49.

Zieman, S. J., Melenovsky, V., Clattenburg, L., Corretti, M. C., Capriotti, A., Gerstenblith, G., & Kass, D. A. (2007). Advanced glycation endproduct crosslink breaker (alagebrium) improves endothelial function in patients with isolated systolic hypertension. *Journal of Hypertension*, *25*(3), 577–583.

How to cite this article: Dobrucki, I. T., Miskalis, A., Nelappana, M., Applegate, C., Wozniak, M., Czerwinski, A., Kalinowski, L., & Dobrucki, L. W. (2023). Receptor for advanced glycation end-products: Biological significance and imaging applications. *WIREs Nanomedicine and Nanobiotechnology*, e1935. https://doi.org/10.1002/wnan.1935